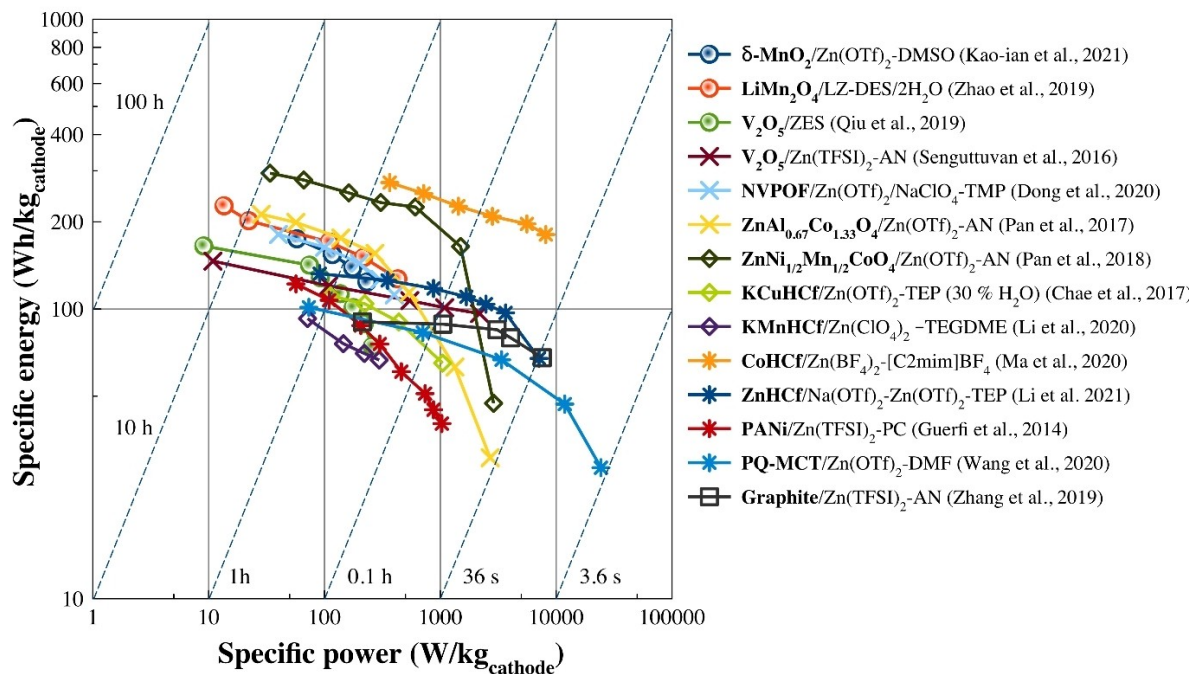
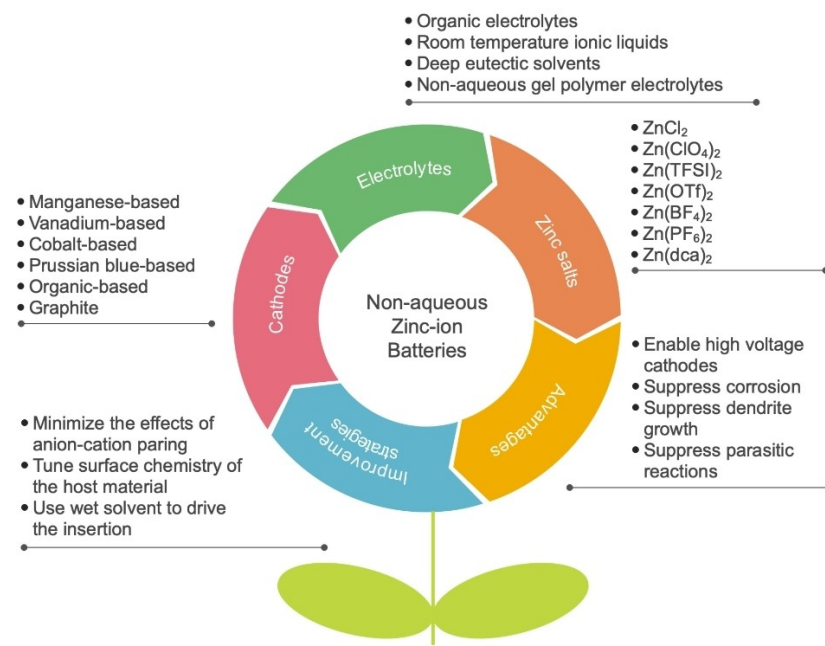


Stability Enhancement of Zinc-Ion Batteries Using Non-Aqueous Electrolytes

Wathanyu Kao-ian,^[a] Ahmad Azmin Mohamad,^[b] Wei-Ren Liu,^[c] Rojana Pornprasertsuk,^[d, e, f, g] Siwaruk Siwamogsatham,^[h] and Soorathee Kheawhom^{*[a, f, i]}



Owing to their high energy density and low cost, zinc-ion batteries (ZIBs) are gaining much in popularity. However, in practice, issues with hydrogen evolution, zinc dendrite development, corrosion, and passivation persist. Such drawbacks prove difficult to eradicate completely. To address these difficulties, many techniques have been proposed including inhibitor addition, artificial SEL, and Zn electrode modification. As a result, some researchers believe that using non-proton donor electrolytes or nonaqueous electrolytes can fundamentally solve these

problems. Herein, the efforts to apply nonaqueous electrolytes such as organic electrolytes, room-temperature ionic liquids, and deep-eutectic solvents to ZIBs are described. An understanding of the mechanisms of nonaqueous ZIBs (NZIBs) regarding zinc plating/stripping and intercalation/deintercalation is also highlighted. Importantly, research gaps are identified in order to pave the way for future study. In addition, an attempt is made to offer a viewpoint on critical topics as well as a benchmarking and enhancement of NZIB technologies.

1. Introduction

At present, due to the enormous demand for efficient energy storage systems (ESSs), battery systems have become one of the hottest topics of research. Even though various systems using lithium-ion batteries (LIBs), Ni-MH batteries, and Pb-acid batteries dominate the ESS market, research into alternative battery systems having additional critical attributes such as safety, sustainability, and eco-friendliness is still ongoing.^[1] Multivalent metals, i.e., zinc (Zn), calcium (Ca), and aluminum (Al), have received much attention for use as battery electrodes owing to their large volumetric capacity (Zn, Mg, Ca and Al: 5851, 3833, 2073, and 8046 mAh/cm³, respectively) as well as their safety, resource availability and nontoxicity.^[2] Nonetheless,

most of them suffer from poor electrochemical reversibility caused by the passive layer formation at solid-liquid interfaces upon dissolution. This shortcoming limits their application in rechargeable batteries. However, through the use of mild-acid electrolytes based on water, reversibility of metallic Zn electrodes can be achieved.^[3] This type of electrolyte has been applied to intercalation type batteries based on Zn, i.e., Zn-ion batteries (ZIBs). As proposed by Xu et al. (2011),^[4] ZIBs utilizing manganese dioxide (MnO_2) and aqueous electrolytes have captured much attention worldwide.

The charge-storage mechanism of ZIBs rely on two processes: namely, the intercalation/deintercalation of Zn^{2+} at cathode, i.e., $xZn^{2+} + 2xe^- + H \leftrightarrow Zn_xH$, where H is host material, or also called intercalation material and the dissolution/deposition of Zn at anode, e.g., $Zn \leftrightarrow Zn^{2+} + 2e^-$, as illustrated in Figure 1. Theoretically, Zn as an electron source, can deliver a large capacity of 820 mAh/g via dissolution reaction. In most cases, the capacity of ZIBs have been limited by the lower capacity of host material.^[3,5] To date, several kinds of host material, i.e., transition metal (Mn, V, Mo, Co and Ni) oxides, transition-metal sulfides, transition-metal phosphates and Prussian blue analogues have been undertaken in the study of ZIBs.

Water-based or aqueous electrolytes, because of their simplicity, non-toxicity and cheapness, are the most widely applied electrolytes in the study of ZIBs.^[6] A variety of Zn salts viz. $ZnSO_4$, $ZnCl_2$, $Zn(ClO_4)_2$, $Zn(NO_3)_2$, $Zn(OTf)_2$, and $Zn(TFSI)_2$ have been used as a Zn^{2+} source.^[3] Generally, electrolytes based on these mentioned salts are neutral or mild-acid, and result in a better surface quality of electrodeposited Zn at the anode and lower self-corrosion than that of alkaline electrolytes.^[7] Aqueous ZIBs (AZIBs) show great potential as a battery system for the next generation. Several AZIBs recently proposed are seen to be very promising both in terms of performance and cyclability viz. those having a specific capacity of more than 200 mAh/g (weight of host material) and achieving thousands of cycles of repeated charging/discharging.^[8] However, up to now, no ZIBs have been recommended for the commercialized battery market.^[2] This outcome points to the fact that there are a number of barriers, which limit their application in practice. According to the literature, the issues within the AZIBs system are as follows:

(I) **Hydrogen evolution reaction (HER):** since water is a protic solvent, which can dissociate and provide proton (H^+), the contribution of H^+ upon charging is unavoidable. Thus, the H^+ reduction reaction $[2H^+(aq) + 2e^- \rightarrow H_2(g); E^\circ =$

- [a] Dr. W. Kao-ian, Prof. S. Kheawhom
Department of chemical engineering, Faculty of engineering
Chulalongkorn University
Bangkok 10330, Thailand
E-mail: soorathee.k@chula.ac.th
- [b] Prof. A. A. Mohamad
School of Materials and Mineral Resources Engineering
Universiti Sains Malaysia
Nibong Tebal, Pulau Pinang 14300, Malaysia
- [c] Prof. W.-R. Liu
Department of Chemical Engineering, R&D Center for Membrane Technology
Research Center for Circular Economy
Chung Yuan Christian University
Chung Li, Taiwan (R.O.C.)
- [d] Prof. R. Pornprasertsuk
Department of Materials Science, Faculty of Science
Chulalongkorn University
Bangkok 10330, Thailand
- [e] Prof. R. Pornprasertsuk
Center of Excellence in Petrochemical and Materials Technology
Chulalongkorn University
Bangkok 10330, Thailand
- [f] Prof. R. Pornprasertsuk, Prof. S. Kheawhom
Research Unit of Advanced Materials for Energy Storage
Chulalongkorn University
Bangkok 10330, Thailand
- [g] Prof. R. Pornprasertsuk
Department of Materials Science and Technology
Nagaoka University of Technology
Niigata, 940-2188, Japan
- [h] Dr. S. Siwamogsatham
National Science and Technology Development Agency
Pathumthani 12120, Thailand
- [i] Prof. S. Kheawhom
Bio-Circular-Green-economy Technology & Engineering Center (BCGeTEC)
Faculty of Engineering
Chulalongkorn University
Bangkok 10330, Thailand

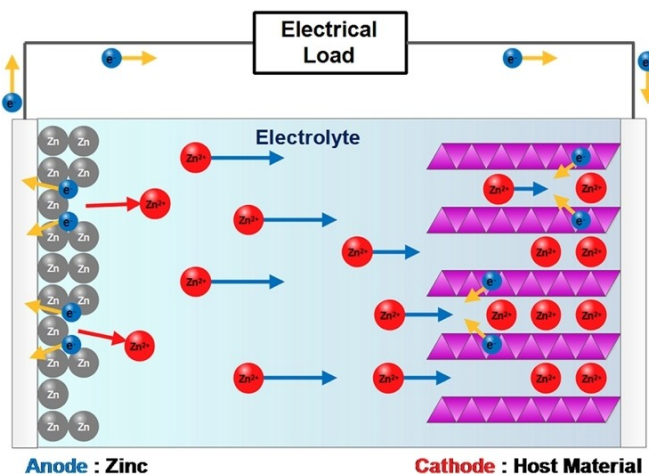
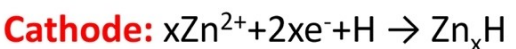
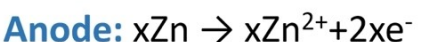


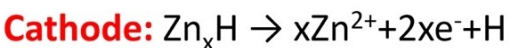
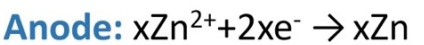
Figure 1. Schema of the charge-storage mechanisms of ZIBs.

0.00 V], also called HER, which generates H₂ gas, is considered to be a competitive reaction resulting in lower charging efficiency and excessive pressure within the battery package.^[9] In practice, the high concentration of

Discharging



Charging



Zn salts, as well as the addition of some inhibitor can suppress HER.^[10]

- (ii) **Dendrite formation:** dendrite formation is not such a new issue in battery research, especially in the system where metallic anodes are used. In AZIBs, Zn dendrites can be



Dr. Wathanyu Kao-ian obtained his B. Eng. degree in Chemical Engineering from King Mongkut's Institute of Technology Ladkrabang in 2015. He then received the Royal Golden Jubilee (RGJ) PhD Program scholarship and completed D.Eng. at Chulalongkorn University in 2022, under the supervision of Prof. Soorathee Kheawhom. He is currently a postdoctoral researcher in Prof. Soorathee Kheawhom's research group. His research focuses on the development of zinc-ion and zinc-iodine batteries.



Dr. Ahmad Azmin Mohamad is an associate professor for School of Materials & Mineral Resources Engineering at Universiti Sains Malaysia. He obtained his doctoral degree in the field of Advanced Materials at physics department, Universiti Malaya. His area of interest focuses on batteries, supercapacitors, and corrosion.



Prof. Wei-Ren Liu is a professor at Chung Yuan Christian University and is leading a research group on "Energy Materials Laboratory." He received his doctor degree in Nation Taiwan University in 2006. He worked as a researcher in Industry Technology Research Institute from 2006 to 2011. His main interests are on lithium-ion batteries, sodium ion batteries, solid-state batteries, graphene-based materials as well as luminescence materials and perovskite quantum dots.



Assoc. Prof. Rojana Pornprasertsuk is currently a faculty member at Chulalongkorn University and remote-crossed appointed associate professor at Nagaoka University of Technology. She received her doctoral degree at Stanford University and started working at Chulalongkorn University since 2007. Her research work focuses on the Zn-based energy storage, fuel cell, primary battery recycled process, synthesis of oxide nanofiber and nanoparticle, ORR catalyst and photocatalyst.



Dr. Siwaruk is a director at National Security and Dual-Use Technology Center, National Science and Technology Development Agency, Thailand. He completed his Ph.D. in Electrical Engineering at The Ohio State University, in 2002. He has focused his research work toward various fields, including wireless, security, embedded systems, and energy storage technologies. His recent notable contributions include establishments of a center of excellence, a pilot production plant, and an industrial consortium on energy storage technologies made of abundantly available and sustainable materials.



Assoc. Prof. Soorathee Kheawhom is an associate professor at the Department of Chemical Engineering, Chulalongkorn University. He received his doctoral degree from the University of Tokyo in 2004. In the same year, he joined the Faculty of Engineering, Chulalongkorn University. His main research focuses on sustainable energy storage technologies i.e., zinc-air batteries and zinc-ion batteries. Currently, he is leading the research cluster on energy storage.

formed due to the uneven Zn-ion flux and electric field above the Zn anode, and can lead ZIBs to failure because of short-circuit.^[11] Moreover, the operating conditions, i.e., current density and areal capacity involves the evolution of Zn morphology and can further lead to the formation of dendritic structure in long-term cycling.

- (III) **Corrosion of Zn:** self-corrosion of Zn is a different scenario from HER.^[10] Due to the fact that aqueous mild-acid electrolytes always contain protons (H^+), and the $H^+ [2H^+(aq) + 2e^- \rightarrow H_2(g); E^\circ = 0.00 V]$ has a higher standard potential than $Zn^{2+} [Zn^{2+}(aq) + 2e^- \rightarrow Zn(s); E^\circ = -0.76 V]$, these H^+ can withdraw the electron from the metallic Zn. Accordingly, Zn is corroded and changed into Zn^{2+} , and pressure is built-up within the cell due to the H_2 produced. Such an outcome can occur at the rest (inactive) state of the battery.
- (IV) **Passivation:** one of the issues concerned in AZIB development is the formation of a passive layer, which can reduce the performance of AZIBs in long-term cycling.^[5,11b] In the most widely used electrolytes such as aqueous $ZnSO_4$ electrolytes, zinc hydroxysulfate [$Zn_4(OH)_6SO_4 \cdot nH_2O$, ZHS] is found to be the main passivation species. ZHS can form well at the local position where H^+ is consumed due to the redox reaction, i.e., HER and H^+ intercalation. At such a position, accumulation of hydroxide ion (OH^-) occurs, which can aggregate with Zn^{2+} , and SO_4^{2-} to form ZHS. Due to the reduction in the amount of active Zn^{2+} and SO_4^{2-} and the passivation effect of the formed layer, performance and charging efficiency of ZIBs are reduced tremendously.

Many approaches have been proposed to solve these issues, e.g., the inhibitor addition, the artificial SEI, the modification of Zn electrode etc.^[12] However, some researchers believe that these approaches are only passive strategies; such problems cannot be entirely eliminated.^[13] Three out of four issues mentioned in AZIB studies involve the existence of H^+ . Accordingly, some researchers believe that these issues can be avoided fundamentally by employing non-proton donor electrolytes or nonaqueous electrolytes. Due to their wide-stability window, nonaqueous electrolytes such as organic electrolytes have been extensively used in LIBs for more than a decade.^[14] In recent years, several efforts have been initiated to apply nonaqueous electrolytes, i.e., organic electrolytes, room-temperature ionic liquids (RTILs) and deep-eutectic solvents (DESs) to ZIBs. Most nonaqueous ZIB (NZIB) studies guarantee that the HER and Zn corrosion can be effectively inhibited.^[9,13,15] Besides, nonaqueous electrolytes are stable enough to be used with high voltage host materials, i.e., Prussian blue analogue, cobalt oxide, polyanion-type phosphates and graphite, which are unstable in aqueous electrolytes.^[16] However, NZIB technologies still lack categorization: a review, an overall picture, a benchmarking and finally, a target. In addition, it is immensely important to clarify what is missing in the research in order to pave the way towards further development and to produce a clear understanding as regards the mechanisms of NZIB reactions. In this review, an attempt is made to provide a perspective with respect to the important issues and a

benchmarking of NZIB technologies in order to make possible the enhancement of NZIBs.

2. Non-Aqueous Electrolytes, Their Stability and Their Transport Properties

2.1. Organic electrolytes

The development of nonaqueous electrolytes for ZIBs originated from basic requirements viz. a wide operation window, noncorrosive and high ionic conductivity. Han et al. (2016)^[17] first introduced the polar-aprotic solvents i.e., acetonitrile (AN), diglyme (G2), propylene carbonate (PC) and N,N-dimethylformamide (DMF), having Zn salts [i.e., $Zn(TFSI)_2$, $Zn(OTf)_2$, $Zn(PF_6)_2$ and $Zn(BF_4)_2$], as an electrolyte for Zn electrodeposition. AN– $Zn(TFSI)_2$ shows very impressive anodic stability (up to ~ 3.8 V vs. Zn/Zn^{2+}), high ionic conductivity (28 mS/cm, 0.5 M), exhibiting $\geq 99\%$ coulombic efficiency upon the deposition/dissolution of Zn. The superior ionic conductivity of AN– $Zn(TFSI)_2$, which is nearly on a par with mild-acid aqueous electrolyte, is due to the weaker coordination between AN and Zn^{2+} than in other solvents, and the highly dissociated anion such as $TFSI^-$. It is also suggested that the key to attain high electrochemical stability for organic electrolytes comprises 1) the choice of solvent and 2) the choice of anion species i.e., $TFSI^-$, OTf^- or others. Such findings have inspired other research groups to explore the new organic electrolyte systems that meet their requirements, such as triethyl phosphate (TEP), trimethyl phosphate (TMP), tetraethylene glycol dimethyl ether and dimethyl sulfoxide (DMSO), as shown in Table 1. A wider stability window means that higher voltage host material can be applied. Thus, organic electrolytes receive much attention among high voltage host materials e.g., Prussian blue analogue, graphite (anion intercalation) and the cobalt oxide developers.

2.2. Room-temperature ionic liquid (RTIL) and deep-eutectic solvent (DES) based electrolytes

RTIL is one class of a room-temperature molten salt, which is formed from a bulky organic cation i.e., imidazolium ion, pyridinium ion, ammonium ion and phosphonium ion and an organic or inorganic anion.^[25] Such groups possess several beneficial basic features such as intrinsic ion conductivity, negligible volatility, high chemical/thermal stability and a wide electrochemical stability window. According to the literature, there are mainly two groups of conventional RTILs being studied in Zn electrodeposition and in Zn battery research, classified by their cation species e.g., alkyl imidazolium and alkyl pyrrolidinium.^[26] Simons et al. (2014)^[27] indicated the possibility of using RTILs in Zn battery applications. 1-ethyl-3-methylimidazolium dicyanamide ($[C_2mim]dca$) and 1-butyl-1-methylpyrrolidinium dicyanamide ($[C_4mpyrr]dca$), containing 3 wt % water and 9 mol % Zn dicyanamide $[Zn(dca)]_2$, have

Table 1. Organic electrolytes in ZIB application.

Name	Zn salts	Host materials	Anodic stability [V vs. Zn/Zn ²⁺]	Conductivity [S/cm]	Ref.
Acetonitrile (AN)	Zn(TFSI) ₂ Zn(OTf) ₂ Zn(ClO ₄) ₂ Zn(PF ₆) ₂ Zn(BF ₄) ₂	V ₂ O ₅ V ₃ O ₇ ·H ₂ O VOPO ₄ ·2H ₂ O PPy-VOPO ₄ δ-MnO ₂ K _x Ni[Fe(CN) ₆] _{1-y} (H ₂ O) _y ZnAl _x Co _{2-x} O ₄ ZnNi _x Mn _x Co _{2-2x} O ₄ Graphite*	2.2–3.8	~10 ⁻²	[16b,c,f,17,18]
Diglyme (G2)	Zn(TFSI) ₂ Zn(OTf) ₂ Zn(PF ₆) ₂ Zn(OTf) ₂ Zn(PF ₆) ₂ Zn(BF ₄) ₂	N/A	2.3–2.6	~10 ⁻³	[17]
Propylene carbonate (PC)	Zn(TFSI) ₂ Zn(OTf) ₂ Zn(PF ₆) ₂ Zn(OTf) ₂ Zn(PF ₆) ₂ Zn(BF ₄) ₂	Polyaniline (PANI)*	3.3–3.4	~10 ⁻³	[17,19]
N,N-dimethylformamide (DMF)	Zn(TFSI) ₂ Zn(OTf) ₂ Zn(PF ₆) ₂ Zn(BF ₄) ₂	Phenanthrenequinone macrocyclic trimer (PQ-MCT)	2.5–2.9	~10 ⁻²	[15a,17]
Triethyl Phosphate (TEP)	Zn(OTf) ₂	Copper hexacyanoferrate (KCuHCF) Zinc hexacyanoferrate (ZnHCF)	2.25	~10 ⁻³	[16a,20]
Trimethyl phosphate (TMP)	Zn(OTf) ₂	Na ₃ V ₂ (PO ₄) ₂ O ₂ F (NVPOF) VS ₂	2.8	~10 ⁻³	[16d,21]
Tetraethylene glycol dimethyl ether (TEGDME) Dimethyl Sulfoxide (DMSO)	(Zn(ClO ₄) ₂) Zn(OTf) ₂	K _{1.6} Mn _{1.2} Fe(CN) ₆ (MnHCF) δ-MnO ₂ α-MnO ₂	N/A 2.0	N/A ~10 ⁻²	[15b] [9,22]
Cosolvent propylene carbonate (PC)/ Triethyl Phosphate (TEP) Cosolvent dimethylamine (DMA)/ Tetrahydrofuran (THF)	Zn(OTf) ₂ Zn(TFSI) ₂	Polytriphenylamine composite (PTPAn) N/A	2.8 N/A	~10 ⁻³ ~10 ⁻³	[23] [24]

*Anion intercalation

been examined as an electrolyte for a Zn symmetrical (Zn/Zn) cell. Although, such work did not demonstrate very good reversibility of Zn at cycling, it proved that the deposition/dissolution of Zn from/into RTIL can exist. Lately, [C₂mim] based RTILs, having different anion species i.e., OTf⁻, BF₄, OAc⁻ have been found in several studies.^[13,16e,28] RTILs have still not received much attention in Zn battery studies; yet they cannot be overlooked.

Another type of RTIL: namely, a deep eutectic solvent (DES), has been formed from a mixture of hydrogen bond donor (HBD) and hydrogen bond acceptor (HBA) i.e., quaternary ammonium salt, leading to a complex formation, and further resulting in the depression of the freezing point.^[29] Abbott et al. (2003)^[30] first introduced DES. Due to the fact that DESs can contain a huge amount of multivalent cations and provide comparable properties as in traditional RTILs, DESs have become one of the interesting solvent choices for ZIBs.^[31] In addition, DESs have proved that they are more environmentally friendly than traditional RTILs. RTIL and DES electrolytes previously studied in Zn batteries are shown in Table 2.

2.3. Non-aqueous gel polymer electrolytes (NAQ-GPEs)

Another form of electrolytes developed for Zn-based batteries is a quasi-solid-state film produced via solution casting of a mixture containing polymer matrix, salt, and plasticizer, called GPE.^[38] GPEs possess higher ionic conductivity range (~10⁻⁴ to 10⁻² S/cm) than solid polymer electrolytes (SPEs, 10⁻⁸ to 10⁻⁵ S/cm). This is due to the combination of both cohesive and diffusive properties. The advantages of GPE over traditional liquid electrolytes are that the GPE can provide better homogeneity of Zn²⁺ migration, minimizing the dendrite formation, higher dielectric constant and higher transference number.^[5,39] Most recently published articles studied aqueous-based GPEs, whilst nonaqueous-based GPEs (NAQ-GPEs) receive less attention.^[38a] However, despite aqueous-based GPEs exhibiting better mass transport than NAQ-GPEs, most NAQ-GPEs show wider operating temperatures.

Table 3 displays a summarized data from articles regarding NAQ-GPE. Polymers namely poly(vinylidene fluoride-co-hexa-fluoropropylene) (PVdF-HFP), polyvinyl chloride (PVC), poly(ethyl methacrylate) (PEMA), poly(ethylene oxide) (PEO) and polyacrylonitrile (PAN) have been applied as the polymer matrix. Earlier reports of NAQ-GPEs proposed the use of organic carbonate (i.e., PC, ethylene carbonate (EC)) as the plasticizer

Table 2. RTIL and DES electrolytes in ZIB application.

Name	Zn salts	Host materials	Anodic stability [V vs. Zn/Zn ²⁺]	Conductivity [S/cm]	Ref.
[C ₂ mim]OTf	Zn(OTf) ₂	Graphite	2.8	~10 ⁻³	[16e]
[C ₂ mim]BF ₄	Zn(BF ₄) ₂	CoHCF	2.3–2.8	~10 ⁻²	[13,28a]
[C ₂ mim]dca	Zn(dca) ₂	N/A	1.95 ^[*]	~10 ⁻² [*]	[27,32]
[C ₄ mpyrr]TFSI	Zn(TFSI) ₂	Expanded graphite (EG)	2.6–2.7	~10 ⁻³	[25,33]
[C ₄ mpyrr]dca	Zn(dca) ₂	N/A	2.0 ^[*]	~10 ⁻² [*]	[27,34]
ChCl/ Urea	ZnCl ₂	δ-MnO ₂	1.4 (vs. metallic Ag in ChCl/Urea)	~10 ⁻³	[35]
Ace/Zn(TFSI) ₂	Zn(TFSI) ₂	V ₂ O ₅	2.4	~10 ⁻⁴	[31b]
Ace/Zn(ClO ₄) ₂	Zn(ClO ₄) ₂	γ-MnO ₂	N/A	~10 ⁻³	[36]
Urea/LiTFSI/Zn(TFSI) ₂	Zn(TFSI) ₂	LiMn ₂ O ₄	2.5 ^[*]	~10 ⁻⁵ (neat) ~10 ⁻³ [*]	[37]

[*] Measured from the solution containing water

Table 3. NAQ-GPEs for Zn based battery

Polymer matrix	Salts and solvent	Highest ionic conductivity [S/cm]	Highest Transference number of Zn ²⁺	Zn plating/ stripping	Intercalation cathode	Anodic limit [V vs. Zn/Zn ²⁺]	Ref.
PVdF-HFP	Zn(OTf) ₂ /[C ₄ mim]OTf	N/A	N/A	No plated Mn on Zn anode (full cell GCD)	MnO ₂ (capacity ~120 mAh/g)	N/A	[40]
PVDF-HFP	Zn(OTf) ₂ /[C ₄ mim]OTf	N/A	N/A	N/A	MnO ₂	N/A	[41]
PVC/PEMA	Zn(OTf) ₂ /[C ₂ mim]TFSI	1.10×10 ⁻⁴	0.63	N/A	N/A	3.23	[42]
PVDF-HFP/PEO	Zn(BF ₄) ₂ /[C ₂ mim]BF ₄	1.69×10 ⁻²	N/A	99.32% CE, smooth Zn (GCD)	CoHCF (capacity ~180 mAh/g)	N/A	[13]
PEO/PVDF	Zn(OTf) ₂ /[C ₂ mim]TFSI	1.63×10 ⁻⁴	N/A	N/A	N/A	N/A	[43]
PVdF-HFP	Zn(OTf) ₂ /[C ₂ mim]TFSI, [C ₄ mim]OTf and [C ₂ mim]OTf	7.07×10 ⁻³	0.53	CV	MnO ₂ (capacity ~120 mAh/g)	N/A	[44]
PVdF-HFP	Zn(OTf) ₂ /[C ₂ mim]TFSI	3.8×10 ⁻³	0.58	CV	MnO ₂ (capacity ~125 mAh/g)	~3.5	[45]
PVDF-HFP	Zn(TFSI) ₂ /[C ₂ mim]TFSI	>1×10 ⁻³	N/A	CV	N/A	5 (without Zn-(OTf) ₂)	[46]
Poly-ε-caprolactone (PCL)	Zn(OTf) ₂ /[C ₂ mim]TFSI	1.1×10 ⁻⁴	0.62	N/A	N/A	2.5	[47]
PVC/PEMA hav- ing SiO ₂	Zn(OTf) ₂ /[C ₂ mim]TFSI	6.7×10 ⁻⁴	0.69	CV	N/A	5.07	[48]
PVDF-HFP PAN	Zn(OTf) ₂ /PC,EC,PEG:DME Zn(OTf) ₂ /PC:EC	1.6×10 ⁻³ 2.6×10 ⁻³	N/A 0.56	CV CV	N/A γ-MnO ₂ (capacity ~100 mAh/g)	2.8 N/A	[49] [50]
PVdF-HFP hav- ing ZnO particle	Zn(OTf) ₂ /PC:EC	>1×10 ⁻³	0.55	N/A	N/A	N/A	[51]

together with Zn salts [i.e., Zn(OTf)₂]. Recent efforts to develop NAQ-GPEs rely on the use of ionic liquids (ILs), such as 1-butyl-3-methylimidazolium trifluoromethanesulfonate ([C₄mim]OTf) and [C₂mim]TFSI as the plasticizer instead of the organic solvents, which result in the improved thermal stability due to the non-volatile property of the ILs.^[38a]

As seen in Table 3, NAQ-GPEs display reasonable electrochemical stability, ionic conductivity and Zn²⁺ transference number. Furthermore, they provide excellent Zn plating/stripping. Thus, GPE is considered a promising choice for the ZIBs.

2.4. Solvated structure and transport properties

The viscosity of the solvent, the concentration of charge-carrier species, and ion size display a vital role in determining the ionic conductivity of the electrolyte.^[5] Besides, the solvation structure of dissolved salt in the electrolyte influences such properties as

well. The electrostatic force between anion and cation is highly affected by ion transport, and it is even significant in the nonaqueous media.^[2] The basic idea to achieve high ionic conductivity is the development of the solvated structure providing high anion-cation dissociation.^[5]

One approach to attain high dissociating capability is the use of solvents that provide strong interaction with Zn²⁺. For example, Han et al. (2016)^[17] reported that the small size O-donor solvents e.g., DMF, PC and G2 shows higher dissociating capability (between Zn²⁺ and TFSI⁻/OTf⁻) than the N-donor solvent such as AN. Nonetheless, it does not mean that all solvents with strong Zn²⁺ interaction exhibit high ionic conductivity. Other factors e.g., viscosity of solvent and Zn salt concentration must be considered as well. Generally, the lower viscosity implies the better mass transport. Furthermore, the effect of anion specie also influences the ion transport. The use of highly disperse anion (e.g., the anion having weak solvent interaction) results in greater Zn²⁺-anion dissociation and higher ion transport. Moreover, the stronger interaction

between Zn^{2+} and solvent leads to higher desolvation energy which decreases the electrochemical reactivity of Zn^{2+} specie at electrode-electrolyte interface.

It is seen that the interaction between solvent and Zn salt on the electrolyte properties is quite complicated. In addition, the data regarding Zn salt-solvent are significantly limited at present. Thus, further investigation, together with a systematic method to examine the electrolyte system, is required.

2.5. Safety of non-aqueous electrolytes

The most concerning aspect regarding the safety of the electrolytes is their flammability.^[52] Upon the operation, the heat is generated in the battery,^[53] and may result in the vaporization of the low boiling point electrolyte. Such an outcome can be the cause of the burning or explosion.^[53] Thus, physical properties involving thermal stability of solvent (i.e., volatility and flash point) should have been considered for the electrolyte selection. Typically, this issue is more minor of a concern for the electrolyte based on ILs, which are neither flammable nor volatile, but very significant in the case of the organic electrolytes.^[38b]

Table 4 demonstrates the data regarding volatility and flashpoint of the organic electrolytes in NZIB studies. It is seen that AN and THF possess very high vapor pressure (at near RT), low boiling point, and low flash point compared to the others. Despite good electrochemical properties of AN electrolyte,^[18a,54] the poor thermal stability would hinder its application in practice. As their low vapor pressure (<1.0 mm Hg), PC, TEP, TMP, TEGDME and DMSO, are much safer.

3. Zn Anode Performance in Non-Aqueous Electrolytes

3.1. Organic electrolytes

3.1.1. Cyanomethane-based electrolytes

The N-donor cyanomethane solvent such as AN has proven to be one of the most promising choices for NZIBs. Han et al. (2016)^[17] highlighted the effect of solvent choice and the effect

of Zn salt choice on the plating/stripping performance of Zn. Thus, it was found that the weak coordination of Zn^{2+} with AN and the low viscosity proved to be the origin of the high mobility of both cations and anions in AN, especially when combined with $Zn(TFSI)_2$. The electrodeposition of Zn on a platinum electrode using $Zn(TFSI)_2$ -AN and $Zn(OTf)_2$ -AN electrolyte provided significantly higher current density, better %CE (>99% upon -1.0 V to upper anodic limit point) and wider anodic limit (>3.5 V, Figure 2a) than the use of other organic electrolytes i.e., G2, PC and DMF based on $Zn(TFSI)_2$ and $Zn(OTf)_2$ salts. Furthermore, the additional redox reaction trend was clearly observed when $Zn(TFSI)_2$ -G2, $Zn(TFSI)_2$ -PC, $Zn(TFSI)_2$ -DMF, $Zn(OTf)_2$ -G2, $Zn(OTf)_2$ -PC, and $Zn(OTf)_2$ -PC were used as electrolytes, whereas in the $Zn(TFSI)_2$ -AN and $Zn(OTf)_2$ -AN samples, there were no such reactions. Such outcomes were also found in the case of $Zn(BF_4)_2$ -AN and $Zn(PF_6)$ -AN. However, details in depth regarding these additional redox reactions, as well as the relationship between electrolyte properties and electrodeposition of Zn, are not given in this work. Chae et al. (2017)^[18e] claimed that 99.9% CE was achieved over the 20th cycle of CV test for the 0.5 M $Zn(ClO_4)_2$ -AN electrolyte, whereas it was lower than 80% for the aqueous electrolyte (0.5 M $Zn(ClO_4)_2$, 0.1 M $ZnSO_4$ and 0.1 M $ZnSO_4$ -water) at the same cycle number; however, Zn-dendrite was found to be unavoidable.

As regards practical performance, galvanostatic charge-discharge (GCD) cycling results are presented. Zhang et al. (2019)^[16f] stated that 99.5% CE upon GCD test (Ti/Zn cell) was achieved via 1 M $Zn(TFSI)_2$ -AN electrolyte (Figure 2b). In addition, Zn/Zn cell having this electrolyte displayed a very stable operation upon 1000 cycles of GCD cycling (0.5 h charge/0.5 h discharge, 0.5 mA/cm²) 1 C; the cycled electrode was found to be dendrite-free and ZnO passivation-free (Figure 2c and d). Likewise, Etman et al. (2020)^[18a] noted that AN having 0.5 M of $Zn(TFSI)_2$ and $Zn(OTf)_2$ provided reversible Zn plating/stripping for over 500 cycles achieving 99.8% CE (current density: 1.25 to 10 mA/cm²); additionally, the AN-Zn-(OTf)₂ demonstrated better cyclability and slightly lower plating-stripping voltage (Figure 2e). Based on both CV and GCD results, the reversible chemistry of Zn in the AN electrolyte is thus substantiated.

Table 4. Safety data of organic solvents used in NZIB research.

Solvent	Vapor pressure [mmHg]	Boiling point [°C]	Flashpoint [°C]	Toxicity (LD50, oral rat)	Ref.
Acetonitrile (AN)	88.8 (25 °C)	81.6	5.55	175 mg/kg	[55]
Diglyme (G2)	2.96 (25 °C)	162	67	4760 mg/kg	[56]
Propylene carbonate (PC)	0.04 (25 °C)	242	135	29.1 mL/kg	[57]
N,N-dimethylformamide (DMF)	3.87 (25 °C)	153	58	2800 mg/kg	[58]
Triethyl Phosphate (TEP)	0.39 (25 °C)	215	115	1600 mg/kg	[59]
Trimethyl phosphate (TMP)	0.85 (25 °C)	197.2	150	840 mg/kg	[60]
Tetraethylene glycol dimethyl ether (TEGDME)	0.0019 (25 °C)	272-277	141	5140 mg/kg	[61]
Dimethyl Sulfoxide (DMSO)	0.60 (25 °C)	189	95	14500 mg/kg	[62]
Tetrahydrofuran (THF)	162 (25 °C)	65	-14.5	1650 mg/kg	[63]

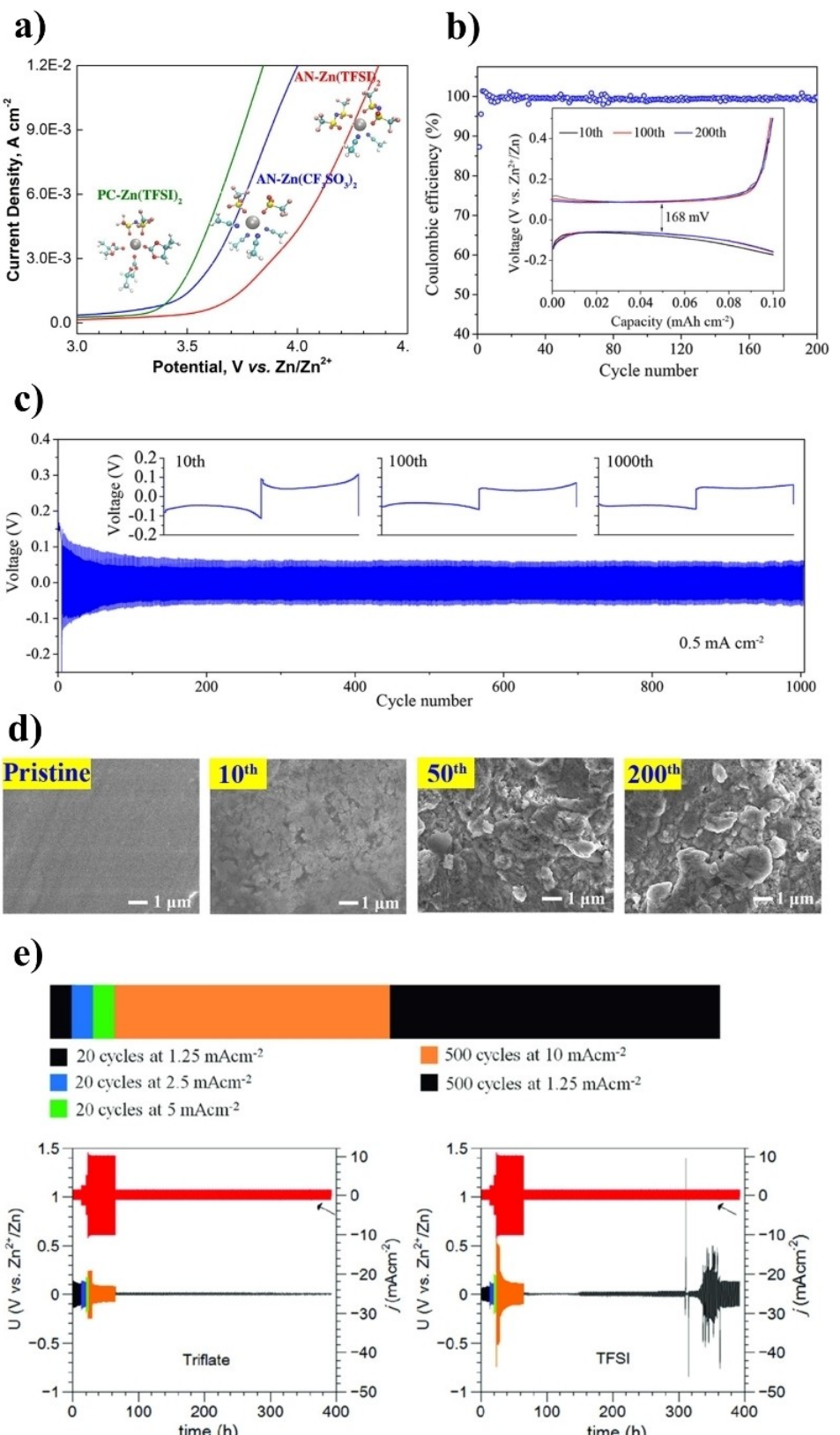


Figure 2. Electrochemical testing results using AN electrolyte: a) Anodic stability of AN and PC electrolytes.^[17] Reproduced with permission from Ref. [17]. Copyright (2016) American Chemical Society. b) Zn plating/stripping testing results using Zn/Ti cell at 0.2 mA/cm² [1 M Zn(TFSI)₂-AN]. c) GCD cycling results using Zn/Zn cell at 0.5 mA/cm² [1 M Zn(TFSI)₂-AN]. d) SEM images of pristine Zn anode and Z anode after 10, 50, 200 cycles.^[16f] Reproduced with permission from Ref. [16f]. Copyright (2019) American Chemical Society. e) GCD cycling results using Zn/Zn cell at 1.25, 2.5, 5, 10 mA/cm² of current density [0.5 M Zn(OTf)₂ vs. 0.5 M Zn(TFSI)₂ in AN].^[18a] Reproduced from Ref. [18a]. Copyright (2020) The Authors. Published by Wiley-VCH GmbH.

3.1.2. Carbonate-based electrolytes

Over the past decade, due to their low-cost, high electrochemical stability and high Li salts solubility, organic carbonate solvents e.g., ethylene carbonate (EC), dimethyl carbonate (DMC), dimethyl carbonate (DEC), ethyl methyl carbonate (EMC) and propylene carbonate (PC) have been extensively used in LIBs.^[14a,4] Guerfi et al. (2014)^[19] revealed the feasibility of using PC as an electrolyte for Zn batteries. However, despite the fact that the Zn/PANI (polyaniline) cell having PC electrolyte (0.3 M Zn(TFSI)₂) possessed high cycling stability, high reversibility of the Zn in PC is observed. Han et al. (2016)^[17] reported the use of PC electrolytes containing Zn(TFSI)₂, Zn(OTf)₂, and Zn(PF₆)₂ achieving ~100% of CE and higher than 3.3 V vs. Zn/Zn²⁺ of anodic limit (Figure 3a). Furthermore, by applying the novel technique called "Zn CE protocols", as proposed by Ma et al. (2020),^[65] the CE value was evaluated more precisely (Figure 3b)

and c). It was found that the PC electrolyte [0.5 M Zn(TFSI)₂] possessed high CE values (99.1, 99.0, 98.8 and 98.0% at current densities of 0.25, 0.5, 1.0, 2.5 mA/cm², respectively) upon GCD Zn deposition/dissolution whereas the water-based electrolyte (1 M ZnSO₄ and 2 M Zn(OTf)₂) could not even pass the test and did not yield any result. In spite of its high CE, the PC electrolyte was not dendrite-free. Furthermore, according to Chen's work,^[66] the PC having Zn(ClO₄)₂ can be used in a Zn/V₂O₅ battery. The battery for the GCD test in this research was set up using a coin cell configuration having a Zn foil anode. It is seen that the full cell passed 5000 cycles of GCD test at high current (10 A/g of V₂O₅), indicating the high cyclability of the Zn anode within this electrolyte system.

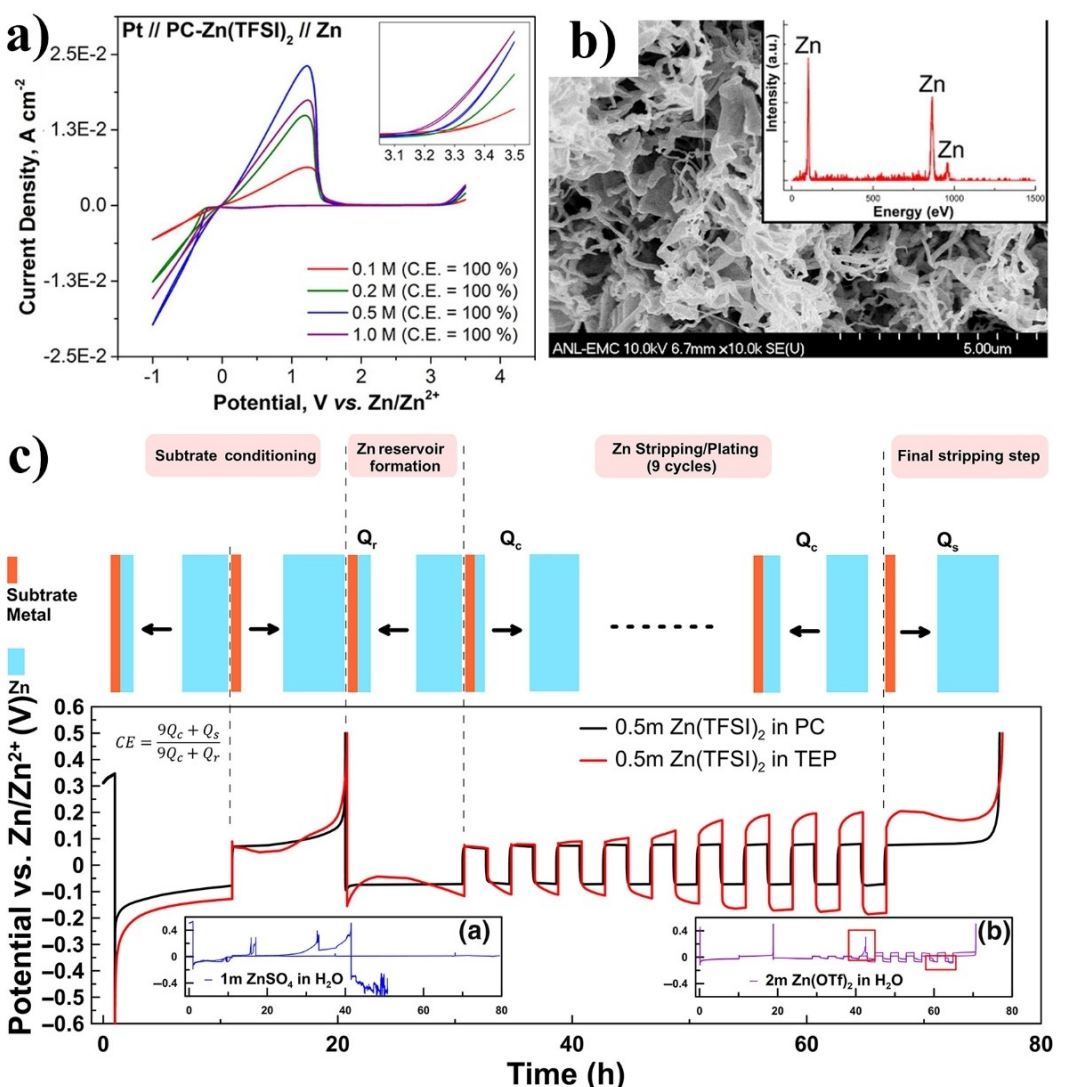


Figure 3. Electrochemical testing results using PC electrolyte: a) CV curves of Pt/Zn(TFSI)₂-PC/Zn cell with various concentration of Zn(TFSI)₂ (0.1–1.0 M). b) Deposited Zn on Pt electrode after deposition overnight [Zn(TFSI)₂-PC].^[17] Reproduced with permission from Ref. [17]. Copyright (2016) American Chemical Society. c) Implementation of Zn CE protocol to the 0.5 M Zn(TFSI)₂-PC, 0.5 M Zn(TFSI)₂-TEP, 1.0 M ZnSO₄-water and 2.0 M Zn(OTf)₂-water.^[65] Reproduced from Ref. [65]. Copyright (2020) Zhengzhou University. Published by Wiley-VCH GmbH.

3.1.3. Amide-based electrolytes

Several Zn salts i.e., $\text{Zn}(\text{TSI})_2$, $\text{Zn}(\text{OTf})_2$, $\text{Zn}(\text{PF}_6)_2$ and $\text{Zn}(\text{BF}_4)_2$ can dissolve in DMF and provide Zn electrodeposition. Han et al. (2016)^[17] reported that only 50.8% of CE was achieved via CV (-1.0 V to upper anodic limit point of ~ 2.8 V) test for the $\text{Zn}(\text{TSI})_2$ -DMF electrolyte. The maximum concentration of $\text{Zn}(\text{OTf})_2$ in DMF was found to be above 1.0 M. The 0.5 M electrolyte yielded the highest ionic conductivity of 18.9 mS/cm and the widest anodic limit of 2.5 V vs. Zn/Zn^{2+} . Wang et al. (2020)^[15a] found that Zn/Zn cell having 0.5 M $\text{Zn}(\text{OTf})_2$ -DMF can pass at least 2800 h of GCD test without failure (1.0 mA/cm 2 having a discharge/charge time of 1.0 h) (Figure 4a). The high CE ($> 99.8\%$) was achieved via SS (stainless-steel)/Zn cell, thus implying the high reversibility chemistry of Zn within the $\text{Zn}(\text{OTf})_2$ -DMF electrolyte. Furthermore, via SEM, it was noted that no dendrite formation upon cycling occurred (Figure 4b).

3.1.4. Phosphate-based electrolytes

Two organic phosphate solvents being used in NZIBs include triethyl phosphate (TEP) and trimethyl phosphate (TMP).^[16a,d] Notably, the dry $\text{Zn}(\text{OTf})_2$ -TEP solution (0.5 M), as an electrolyte, is seen to provide stable cycling of 3000 h via Zn/Zn cell-GCD test at 0.1 – 0.5 mA/cm 2 of current density; the high CE (99.86% at 0.5 mA/cm 2) attained 1000 cycles via SS/Zn cell-GCD test, and wide anodic limit (2.25 V vs. Zn/Zn^{2+})^[16a] (Figure 5a and b).

Besides, the Zn/Zn cell having this electrolyte can pass a long-period of cycling (10 h Charge/ 10 h Discharge, 0.5 mA/cm 2) and can last for 2000 h of total time. The main morphology of Zn after cycling was found to be a cage-like porous network (Figure 5c); this kind of Zn morphology came about by following an in-situ-formed molecular template, which was initiated by the $\text{Zn}_3(\text{PO}_4)_2$ layer between the Zn-electrolyte interface. However, the full cell, having dry TEP electrolyte and Prussian blue cathode, was not successful at cycling; there was an electrolyte modification by adding water into the electrolyte. It is noted that adding water into the solvent formed the 7:3-TEP:water by volume such that it enhanced the full cell cyclability tremendously. However, it also reduced the CE of Zn anode and the anodic limit of the electrolyte.

According to Naveed et al. (2019),^[21] Zn can also be deposited through the TMP electrolyte that contained $\text{Zn}(\text{OTf})_2$. The TMP electrolyte [0.5 M $\text{Zn}(\text{OTf})_2$ -TMP] provided not only a high CE value (99.57% via SS/Zn cell-GCD test), but also exhibited very stable plating/stripping via Zn/Zn cell-GCD test ($> 2,000$ h at 0.1 , 0.25 , 0.5 and 1.0 mA/cm 2). In addition, 1000 h of rigorous GCD tests, having 10 h of charge/discharge time and 0.5 – 1 mA/cm 2 of current density, were achieved using this electrolyte. The main Zn morphology developed upon cycling was found to be a graphene-like porous structure, which allows for the high rate of Zn plating/stripping and the facile Zn^{2+} transport. This kind of Zn structure was formed by a mechanism similar to that of the TEP electrolyte.

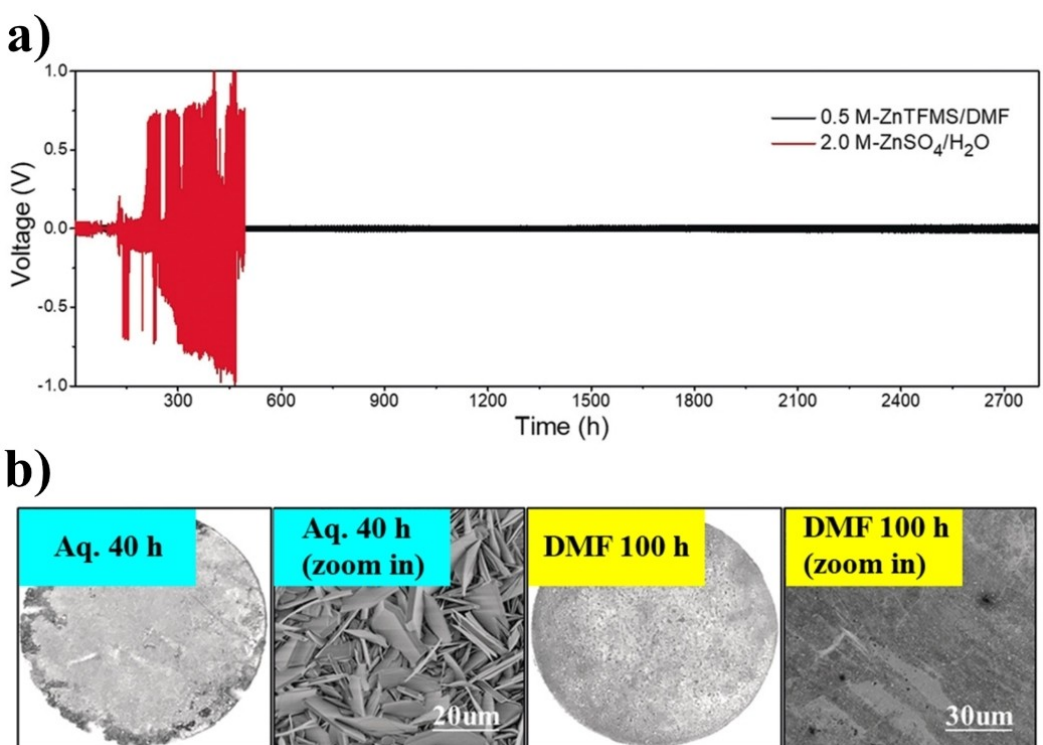


Figure 4. a) GCD cycling results of Zn/Zn cell having 0.5 M $\text{Zn}(\text{OTf})_2$ (TFMS)-DMF and 2.0 M ZnSO_4 -water electrolytes at 1.0 mA/cm 2 . b) SEM images of cycled electrodes at 1.0 mA/cm 2 (light blue: 2.0 M ZnSO_4 , 40 h cycling time) [yellow: 0.5 M $\text{Zn}(\text{OTf})_2$ -DMF, 100 h cycling time].^[15a] Reproduced with permission from Ref. [15a]. Copyright (2020) Wiley-VCH.

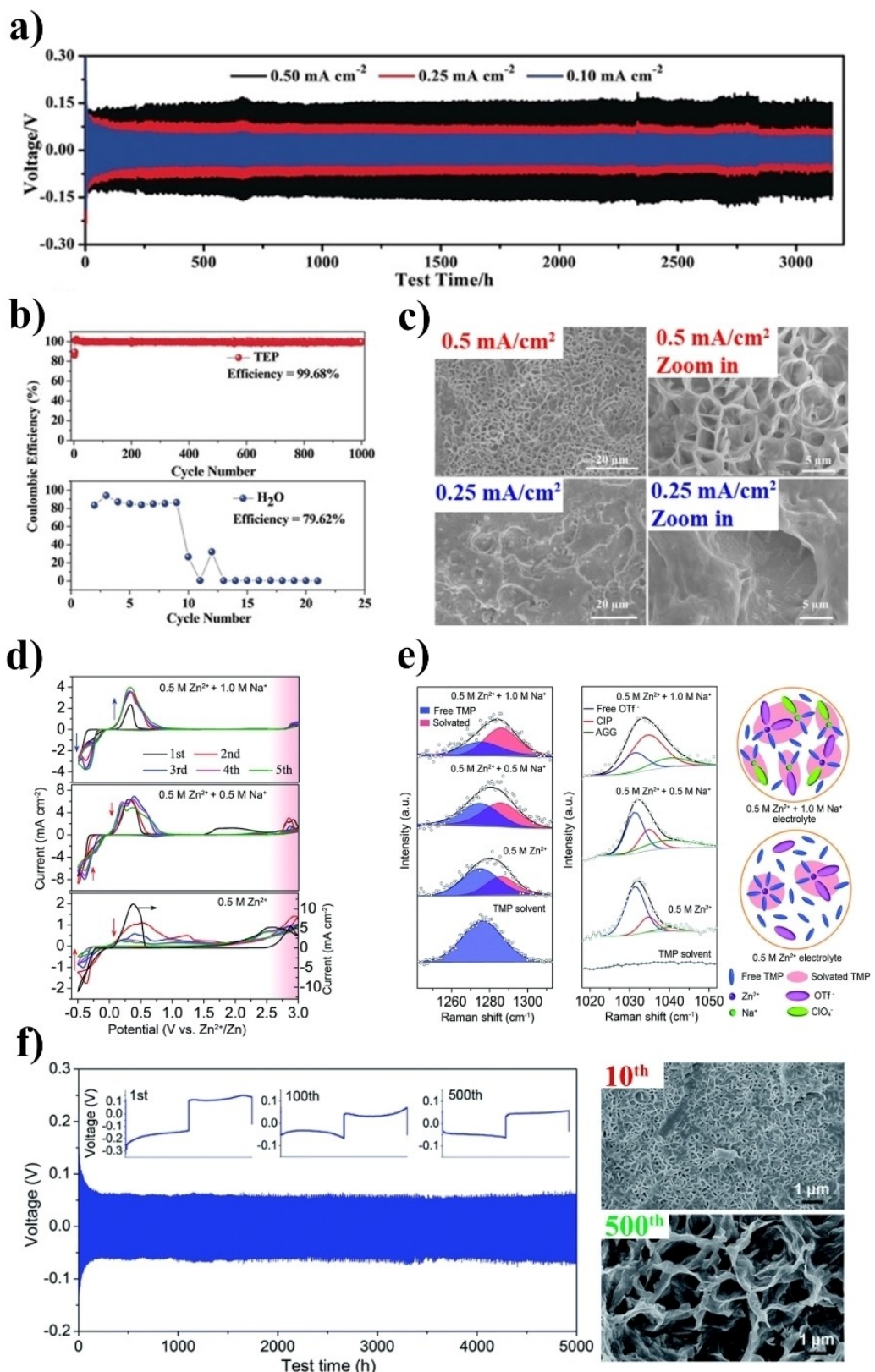


Figure 5. Phosphate-based electrolyte in action: a) GCD results of Zn/Zn cell having 0.5 M Zn(OTf)₂-TEP at 0.1–0.5 mA/cm². b) CE values obtained from GCD test (0.5 mA/cm²) of SS/Zn cell [0.5 M Zn(OTf)₂ in TEP vs. in water]. c) SEM images of cycled (2000 h) electrode using 0.5 and 0.25 mA/cm² current density.^[16a] Reproduced with permission from Ref. [16a]. Copyright (2019) Wiley-VCH. d) Cyclic voltammogram of Ti/Zn cell having 0.5 M Zn(OTf)₂/1.0 M NaClO₄-TMP, 0.5 M Zn(OTf)₂/0.5 M NaClO₄-TMP, and 0.5 M Zn(OTf)₂-TMP electrolytes, respectively, from top to bottom. e) Raman spectra in the region from 1242 to 1313 cm⁻¹ (left) and from 1020 to 1050 cm⁻¹ (middle), and schematic simulates the solvated species in electrolyte. f) GCD results of Zn/Zn cell having 0.5 M Zn(OTf)₂/1.0 M NaClO₄-TMP at 0.5 mA/cm² and SEM image of cycled electrode after 10th and 500th cycles.^[16d] Reproduced with permission from Ref. [16d]. Copyright (2020) The Royal Society of Chemistry.

However, Dong et al. (2020)^[16d] noted that Zn(OTf)₂-TMP electrolyte is unstable when operated at a high voltage. To overcome such an issue, a CV test was performed using a higher upper potential limit (−0.6 to 1.25 V vs. Zn/Zn²⁺) than what it was in Naveed's research (−0.5 to 3.0 V vs. Zn/Zn²⁺). As a result, deterioration of the current was observed in the 0.5 M Zn(OTf)₂-TMP sample after only a few cycles of the CV test (Figure 5d). Dong et al. also indicated that this issue can be effectively suppressed using NaClO₄ as an electrolyte additive. Furthermore, at 0.5 M/1.0 M of Zn(OTf)₂/NaClO₄ concentration in TMP, both electrochemical stability and thermal stability can be tremendously enhanced (anodic limit: from 2.0 V to 2.8 V). The characterization e.g., FTIR and Raman results showed that the NaClO₄ addition resulted in reducing free solvents and free anions, thus leading the electrolyte to be more stable (Figure 5e). In addition, the Zn/Zn cell passed 5000 h of total time via the GCD test at 0.5 mA/cm² of current density, and an average 99.8% CE was achieved over 1000 cycles (0.2 mA/cm², 1 h of deposition time) of Ti/Zn cell-GCD test (Figure 5f). After cycling, no Zn dendrite was observed.

3.1.5. Ether-based electrolytes

The ether-based solvent such as G2, which contains Zn(TFSI)₂, Zn(OTf)₂, and Zn(PF₆)₂, can provide Zn deposition/dissolution. However, according to Han's work,^[17] it was found that there was a relatively large trend of additional redox reaction as contributed by the Zn plating/stripping CV test. Only one couple, Zn(PF₆)₂-G2 reported 100% CE via the CV test. As yet, to the best of our knowledge, no more reports regarding the use of G2 as an electrolyte for ZIBs have been found.

Tetraethylene glycol dimethyl ether (TEGDME) is viewed as one of the possible solvent choices. However, little is known about TEGDME as an electrolyte for NZIB or for Zn electrodeposition. One example that has been demonstrated is the Li group's work^[15b] whereby metallic Zn foil was used as an anode and K_{1.6}Mn_{1.2}Fe(CN)₆ was used as a cathode. It was found that the battery can pass 8,500 cycles of full cell-GCD at 200 mA/g of current density: this outcome indicated the high reversibility of Zn in the TEGDME electrolyte. In addition, the cycled Zn electrode was found to be smooth and dendrite-free.

3.1.6. Sulfoxide-based electrolytes

One of the possible solvent choices for a Zn battery electrolyte is dimethyl Sulfoxide (DMSO), which possesses several promising properties i.e., high dielectric constant (46.45), high donor number, wide electrochemical window (−2.9 to +1.5 V vs. SCE) and low toxicity. Kao-ian et al. (2021)^[9] demonstrated the application of DMSO in NZIB. By conducting CV experiments, it was found that Zn can plate/strip from/into the Zn(OTf)₂-DMSO electrolyte. In spite of the low CE achieved through the CV test, the SS/Zn cell having the DMSO electrolyte [0.25 M Zn(OTf)₂] exhibited 99.6% according to the GCD cycling test. Furthermore, rate performance proved to be satisfactory via the Zn/Zn

cell-GCD test (61, 63, 73, and 93 mV of Zn plating overpotential at 0.1, 0.2, 0.5 and 1.0 mA/cm² of current density, respectively). Although only 100 h of total time was recorded via the Zn/Zn cell-GCD test, the fact that the full cell (Zn/MnO₂) cycled up to 1000 cycles reflects the high reversibility of Zn anode in the DMSO electrolyte.

3.1.7. Mixed-solvent electrolytes

Mixing is one approach that can be made in order to enhance the properties of an electrolyte. For example, it is acknowledged that PC has a high dielectric constant, but low Zn(OTf)₂ solubility. Qiu et al. (2021)^[23] noted that adding a high O-donor solvent such as TEP into a PC electrolyte can increase its Zn(OTf)₂ solubility limit (0.08 to >0.5 M), anodic limit (2.42 to 2.8 V) and ionic conductivity (1.2 to max. 9.9 mS/cm for TEP:PC = 1:2 sample), and decrease flammability (Figure 6a and c). In addition, it is seen that via the CV test, the TEP/PC electrolyte provided a higher Zn plating/stripping current density than that of the pure TEP and pure PC electrolytes; the TEP:PC = 1:2 was found to be the best ratio (Figure 6b). Hence, the Zn/Zn cell passed 2600 h of GCD at 0.5 mA/cm² of current density and 0.5 mAh/cm² of tested capacity having 0.25 V of voltage polarization. As for SS/Zn cell-GCD test, 97.7% and 99.7% was achieved at current density 0.1 mA/cm² and 5 mA/cm², respectively. A porous inter-connected Zn was found to be the main Zn morphology formed upon the cycling.

Tetrahydrofuran (THF) is an ether solvent, which has low Zn(TFSI)₂ solubility. Nevertheless, it is noted by Genevieve et al. (2021) that adding dimethylamine (DMA) as a cosolvent can increase the Zn(TFSI)₂ solubility.^[24] Thus, Zn(TFSI)₂ solubility, ionic conductivity and deposition/dissolution kinetics of Zn were enhanced (Figure 6d); this improvement occurred as a consequence of the redissociation mechanism. By using 0.3 M Zn(TFSI)₂ 2.0 M DMA in THF as an electrolyte, maximum CE (97%) was achieved via the CV test. It is observed that Zn morphology depends on the amount of DMA used (Figure 6e). Platelet and granular structure of Zn was found when 2.0 and 0.5 M DMA electrolytes were used: higher DMA content results in higher crystallinity of deposited Zn.

The promising features of the TMP electrolyte can further be enhanced using the cosolvent DMC.^[21] When DMC is mixed with TMP in 1:1 volumetric ratio, 0.5 M Zn(OTf)₂-TMP:DMC (1:1) is formed. Thus, it is seen that in comparison with the 0.5 M Zn(OTf)₂-TMP viscosity was reduced, and ionic conductivity increased (4.58 to 4.90 mS/cm). Furthermore, such an approach can enhance both cycling stability (twice longer than the pristine electrolyte) and rate performance. Besides, the TMP electrolyte can be improved by adding DMF (1:1 by volume), which gives similar results compared to the DMC addition.

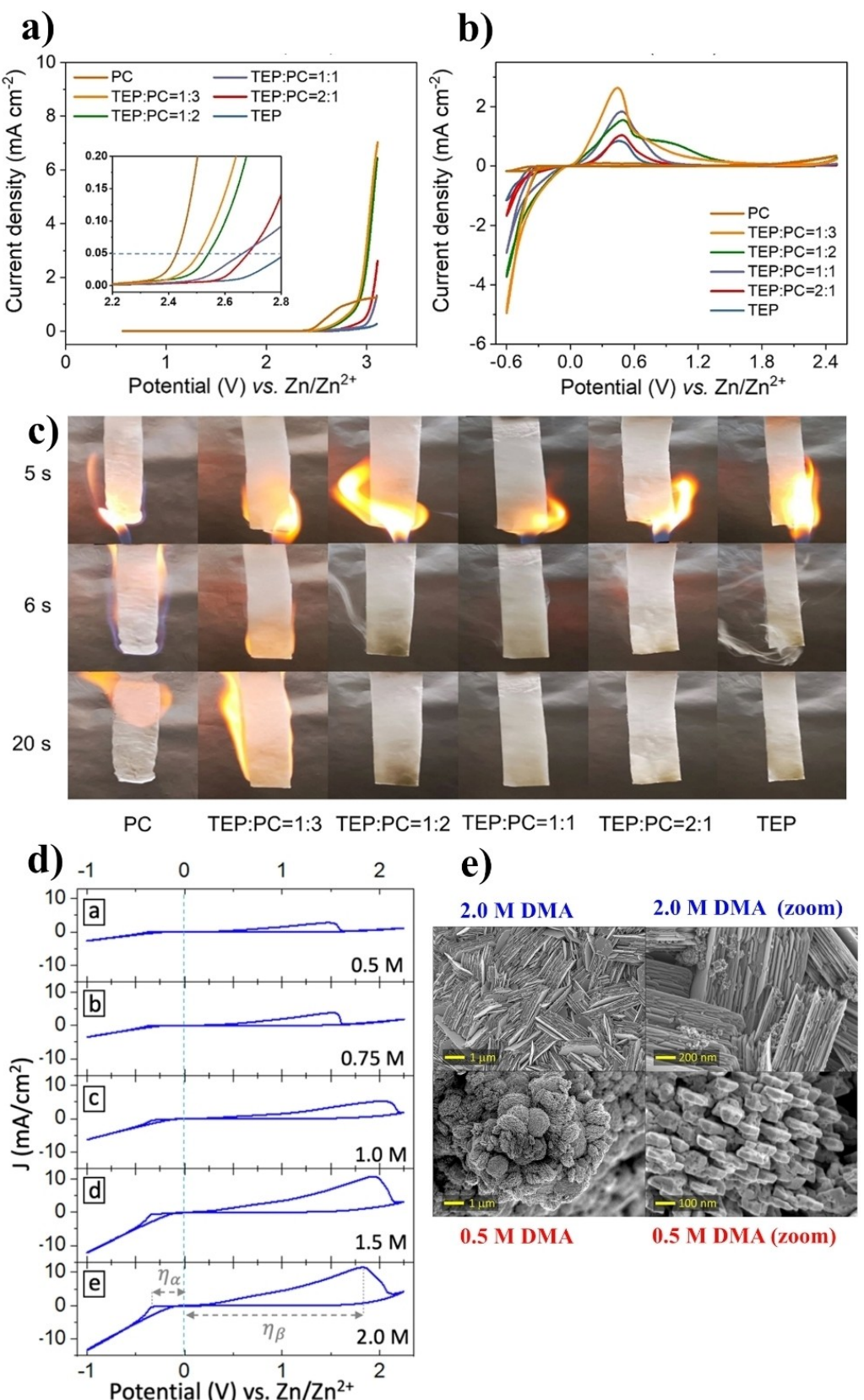


Figure 6. a) Stability window of PC, TEP and TEP:PC (1:3, 1:2, 1:1 and 2:1). b) Cyclic voltammograms (1 mV/s) of PC, TEP and TEP:PC (1:3, 1:2, 1:1 and 2:1) which contained $\text{Zn}(\text{OTf})_2$. c) Flammability test for PC, TEP and TEP:PC (1:3, 1:2, 1:1 and 2:1).^[23] Reproduced with permission from Ref. [23]. Copyright (2021) Wiley-VCH. d) Cyclic voltammograms (50 mV/s) of 0.2 M $\text{Zn}(\text{TFSI})_2\text{-THF}$ at different concentrations of DMA (0.5–2.0 M). e) SEM images of plated Zn from 0.2 M $\text{Zn}(\text{TFSI})_2\text{-THF}$ with different concentration of DMA (0.5–2.0 M).^[24] Reproduced from Ref. [24]. Copyright (2021) The Author(s). Published on behalf of The Electrochemical Society by IOP Publishing Limited.

3.2. RTILs and DESs

3.2.1. Alkyl imidazolium electrolytes

Alkyl imidazolium i.e., 1-methylimidazolium (mim), 1-ethyl-3-methylimidazolium (C_2 mim), 1-ethylimidazolium (eim) is a five-membered N-contained heterocyclic molecule, which carries one positive charge; generally, it appears in the form of salts having one anion e.g., Cl^- , OAc^- , dca, BF_4^- , TFSI $^-$, OTF $^-$ and others. Alkyl Imidazolium salts, which have a melting point lower than room-temperature are classified as RTILs. Due to their heterocyclic structure, imidazolium ILs are found to be thermally and electrochemically stable.^[26] According to the literature, several alkyl imidazolium ILs can dissolve Zn salt, having the same anion species i.e., $Zn(OTf)_2$ in $[C_2mim]OTf$ and can provide Zn deposition.

One of the most applied alkyl imidazolium ILs in Zn battery researches is C_2 mim. Simons et al. (2012)^[27] stated that wet (3 wt% water) $[C_2mim]$ dca containing $Zn(dca)_2$ is more effective at Zn/Zn cell-GCD cycling than that of the alkyl pyrrolidinium such as $[C_4mpyrr]$. 95 cycles i.e., 375 h of total cycling time at 0.1 mA/cm 2 current density were achieved using the wet $[C_2mim]$ dca electrolyte whereas the wet $[C_4mpyrr]$ dca sample passed only 15 cycles (0.05 mA/cm 2 , ~60 h total). Via CV test of Zn stripping/plating, the wet $[C_2mim]$ dca sample provided superior CE (85%) than that of the wet $[C_4mpyrr]$ dca sample (37%). It was also noted that the Zn deposition within the wet $[C_4mpyrr]$ dca electrolyte required a high overpotential of -0.84 vs. Zn/Zn^{2+} , which is much greater than what it was in the wet $[C_2mim]$ dca electrolyte (-0.23 V vs. Zn/Zn^{2+}). However, the dendrite formation of Zn, which led to the failure at cycling was observed in the wet $[C_2mim]$ dca sample after 375 h of the GCD test. Consequently, in spite of the superior testing results of $[C_2mim]$ dca than that of $[C_4mpyrr]$ dca, the $[C_2mim]$ dca was still not fit enough for use in the practical NZIB. Nevertheless, such an outcome proved that the $[C_2mim]$ ILs were able to provide the Zn recharge.

Another $[C_2mim]$ IL founded in Zn battery application is $[C_2mim]OTf$.^[16e] The $[C_2mim]OTf$ containing 0.2 M of $Zn(OTf)_2$ demonstrated 7.3 mS/cm of ionic conductivity, and 2.8 V vs. Zn/Zn^{2+} . However, when $Zn(OTf)_2$ concentration increased, ionic conductivity diminished due to the increase in viscosity. Moreover, the Cu/Zn/Zn cell-CV test, Cu/Zn cell-GCD test, XRD and EDS reflected that via this electrolyte, Zn deposition/dissolution still existed (Figure 7a-c). Plating and stripping overpotential at 0.4 mA/cm 2 upon GCD was found to be -0.3 V and 0.3 V, respectively. According to the SEM result (Figure 7d) of the cycled electrode (GCD: 10 cycles, Chg time 0.5 h), there was no sign of dendrite formation. However, the long-term cycling stability of Zn in this electrolyte was not evident.

$Zn(BF_4)_2-[C_2mim]BF_4$ is one of the most fascinating RTIL electrolytes.^[13] Due to its high $Zn(BF_4)_2$ solubility, which is far superior to most of RTILs (at least 2 M), the $[C_2mim]BF_4$ possessed high ionic conductivity (16.9 mS/cm). In addition, it also has a wide anodic limit (2.8 V vs. Zn/Zn^{2+}). As noted by Ma et al. (2020),^[13] the Zn/Zn cell having 2 M $Zn(BF_4)_2-[C_2mim]$ passed 1500 h (3,000 cycles) of GCD test at 2 mA/cm 2 of current

density without dendrite formation (Figure 7e). 99.36% CE was achieved via SS/Zn cell-GCD test at current density of 0.5 mA/cm 2 and charging capacity of 0.5 mAh/cm 2 . Further, by varying the current density, the CE still attained 98.5% even at very low or very high current densities (0.2 to 10 mA/cm 2) (Figure 7f); this reflected the wide operating range of the Zn anode in the $Zn(BF_4)_2-[C_2mim]$ electrolyte.

3.2.2. Alkyl pyrrolidinium electrolytes

Alkyl pyrrolidinium ILs are other heterocycles, which have been extensively studied among LIB developers; this is due to several attractive properties such as high reductive stability, low vapor pressure and incombustibility.^[67] Data regarding the Zn electrodeposition and the Zn batteries of these ILs, however, are still limited. Deng et al. (2011)^[68] was first to apply $[C_4mpyrr]dca$, one of the alkyl pyrrolidinium ILs, in Zn deposition study. The study affirmed that a smooth Zn surface can be produced via the $ZnCl_2-[C_4mpyrr]dca$ electrolyte. Subsequently, Simon et al. (2014)^[27] investigated the $[C_4mpyrr]dca$ containing $Zn(dca)_2$. Thus, an attempt at cycling the Zn/Zn cell using 9 mol% $Zn(dca)_2$ /3 wt% water- $[C_4mpyrr]dca$ electrolyte was carried out at a current density of 0.05 mA/cm 2 and a charge/discharge time of 2 h. However, only 15 cycles and a large voltage hysteresis (>200 mV) were achieved. Such a poor outcome was thought to be due to short-circuit.

Another alkyl pyrrolidinium IL based electrolyte found in the literature was $[C_4mpyrr]TFSI$. Ji et al. (2020)^[33a] stated that the $[C_4mpyrr]TFSI$ can be used as an electrolyte in a Zn/expanded-graphite dual-ion battery. Both 1 M of $Zn(TFSI)_2$ and 2 wt% of ethylene sulfite were added into the $[C_4mpyrr]TFSI$ to form the electrolyte solution. The mixture had an anodic limit of about 2.6 V; 86% capacity retention and 500 cycles of full cell-GCD (at 2 C) were achieved. According to the characterization results of before/after cycling Zn anode, it was found that there was a trace of SEI that formed upon the GCD cycling. The main component of SEI was found to be C, S, F, and O, which attributed to the decomposition of the electrolyte. It is noted that the formed SEI had a role in protecting the electrode from degradation. Besides, the cycled Zn electrode was found to be dense and smooth, and no dendrite detected.

3.2.3. Choline-based DES electrolytes

Quaternary ammonium salt, namely, choline chloride (ChCl) is the basic ingredient of choline-based DES. To form the eutectic solvent, ChCl, as an HBA, was mixed with HBD such as urea, ethylene glycol (EG), glycerol, acetamide (Ace) and other HBDs at a specific ratio. The Zn plating/stripping was made using Zn salts (e.g., $ZnCl_2$) and contained DES.^[31a] The ChCl DES such as ChCl:EG, having 1:2 mole ratio (12CE or Ethaline 200) and containing $ZnCl_2$, has gained much attention for use as an electrolyte in anti-corrosive coating studies.^[69] It was found that nano-sized, smooth and less corrosive Zn was achieved using a 12CE electrolyte.^[70]

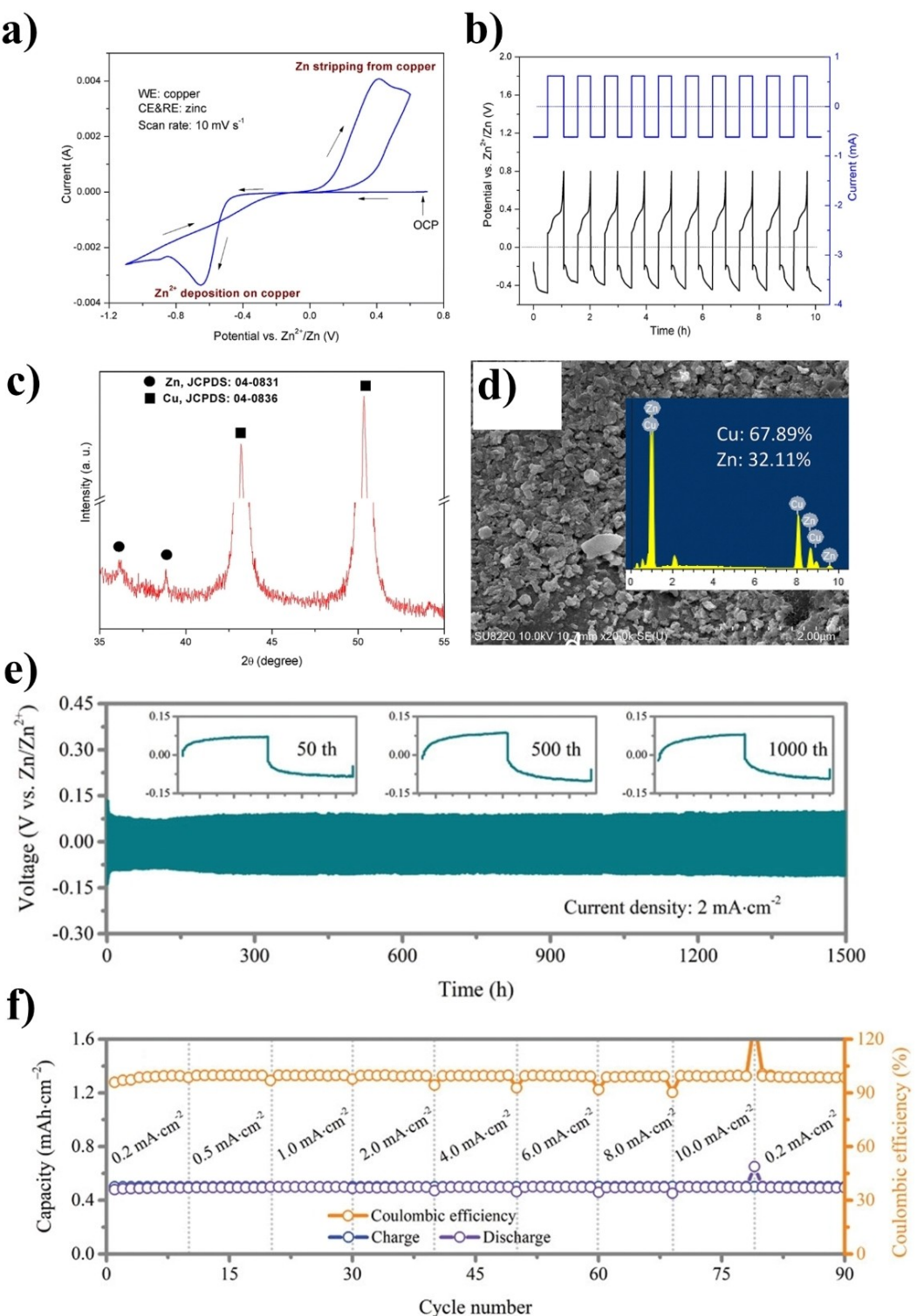


Figure 7. a-d) Anode testing results for 0.2 M of $Zn(OTf)_2\text{-}[C_2mim]OTf$ electrolyte: a) CV curves of Cu/Zn cell at scan rate 10 mV/s. b) GCD cycling results of Cu/Zn cell (10 cycles). c) XRD results of cycled electrode. d) SEM-EDS result of cycled electrode.^[16e] Reproduced with permission from Ref. [16e]. Copyright (2018) Springer-Verlag GmbH Germany, part of Springer Nature. e and f) Anode testing results for 2.0 M $Zn(BF_4)_2\text{-}[C_2mim]BF_4$; e) GCD cycling results of Zn/Zn cell at 2 mA/cm². f) GCD cycling results of SS/Zn cell upon current density range of 0.2–10.0 mA/cm².^[13] Reproduced with permission from Ref. [13]. Copyright (2020) Wiley-VCH.

In the literature, it is acknowledged that 12CE electrolytes have the following features: high ionic conductivity, low viscosity, stability in air and moisture and a wide-electro-

chemical window.^[31a] However, Vieira et al. (2014) found that the Zn deposition process within 12CE electrolytes involved a

Zn-ion complex formation step, which provided H₂ as a byproduct.^[71] The choice of using 12CE proved unsatisfactory.

Another choline-based DES found in the literature is ChCl:urea having 1:2 molar ratio (12CU). The 12CU possesses the ability to dissolve a variety of metal oxides e.g., ZnO, CuO, MnO₂ etc. Using 12CU containing ZnO or ZnCl₂, Zn deposition could be made.^[72] According to the Yang group's research,^[72] although ZnO-12CU can provide smooth and dense deposited Zn, it is seen that the Zn deposition using ZnO-12CU required high temperature (10–100 °C) to increase the solubility of ZnO in 12CU; thus, the ZnO-12CU couple did not suit the Zn battery application. However, the 12CU having ZnCl₂ was able to deposit Zn at room-temperature. According to Kao-ian et al. (2019),^[35a] when 0.3 M ZnCl₂-12CU electrolyte was used, 98% of charge-transfer ratio, calculated from the area under the CV curve (± 0.5 V vs. OCV), was obtained, indicating high reversible Zn plating/stripping (Figure 8a). Yet, large plating/stripping overpotential was found upon the rate performance test (57, 89, 146 and 200 mV at 0.1, 0.2, 0.5 and 1.0 mA/cm², respectively). Only 40 h of total time on the Zn/Zn cell-GCD test was spent on this work (Figure 8b). The morphology of Zn found after the Zn/Zn cell-GCD cycling was a small sphere-grain (~100 nm) (Figure 8c). It was noted by Abbott et al. (2011)^[69a] that due to the fast nucleation of Zn in the ZnCl₂-12CU electrolyte, the Zn grains, which evolved on the deposited layer upon deposition were small.

3.2.4. Acetamide-based DES electrolytes

An acetamide (Ace) can form eutectic mixtures with some Zn salts, resulting in HBAs such as Zn(ClO₄)₂, Zn(TFSI)₂ and ZnCl₂. Venkata Narayanan et al. (2010)^[36] reported the use of Zn(ClO₄)₂:Ace as an electrolyte in Zn/MnO₂ battery. Thus, it was found that due to the lower fraction of ion pairs of the 0.2 Zn(ClO₄)₂: 0.8 Ace (by mole) mixture than others, as observed via FT-IR and FT-Raman, the 0.2 Zn(ClO₄)₂: 0.8 Ace mixture yielded the highest ionic conductivity (6.3 mS/cm), and this fraction was chosen to conduct further tests. By conducting CV on the Zn/Zn cell using 0.2 Zn(ClO₄)₂: 0.8, it was noted that Zn plating/stripping was found to exist and was highly reversible.

Qiu et al. (2019)^[31b] introduced one of the most promising DES electrolytes for Zn batteries viz. Zn(TFSI)₂:Ace (1:4 by mole, called ZES). Subsequently, the electrolyte structure analysis revealed that the solvate structure of Zn in ZES was [ZnTFSI_m(Ace)_n]^{(2-m)+} (where $m=1-2$, $n=1-3$) (Figure 9a). This solvated structure provided the formation of anion-derived SEI on the Zn anode upon the plating. It is acknowledged that SEI played an important role in controlling the shape of deposited Zn (Figure 9b) viz. preventing dendrite and minimizing self-discharge, and finally featuring the high ionic conductivity (2.36 × 10⁻⁶ S/cm). Via Zn plating/stripping CV tests, an average CE of 99.7% over 200 cycles was achieved. Furthermore, the Zn/Zn cell steadily cycled up to 2,000 cycles of GCD cycling (at 0.05 mAh/cm² of testing capacity and 0.1 mA/cm² of current density) (Figure 9c). Upon applying a higher current (1 mA/cm²) and a capacity of (0.5 mAh/cm²) GCD cycling, the Zn/Zn cell

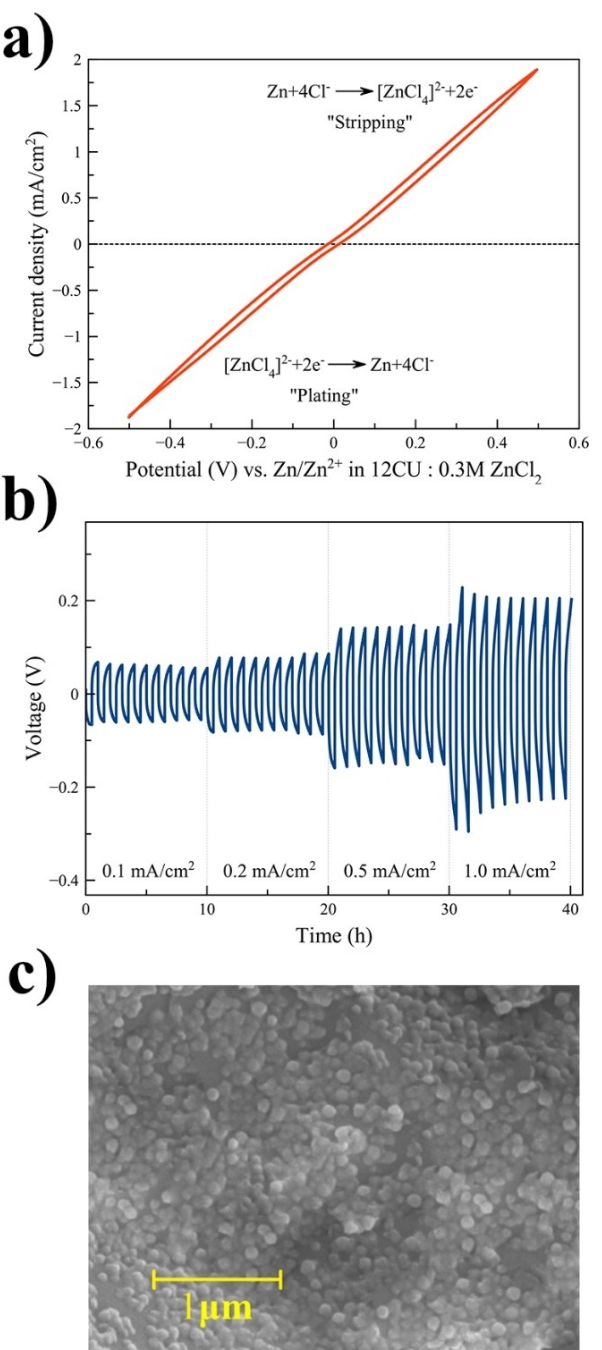


Figure 8. Electrochemical performance of Zn anode within 0.3 M ZnCl₂-12CU electrolyte: a) CV curves of Zn/Zn cell at 10 mV/s (± 0.5 V vs. OCP). b) GCD cycling results of Zn/Zn cell at various current densities (0.1–1.0 mA/cm²). c) SEM image of the cycled Zn anode.^[35a] Reproduced from Ref. [35a]. Copyright (2019) The Author(s). Published by ECS.

operated for at least 100 h. In addition, it is noted that SEI can maintain the uniform and dendrite-free Zn deposition even at the higher capacity (2.5–5 mAh/cm²).

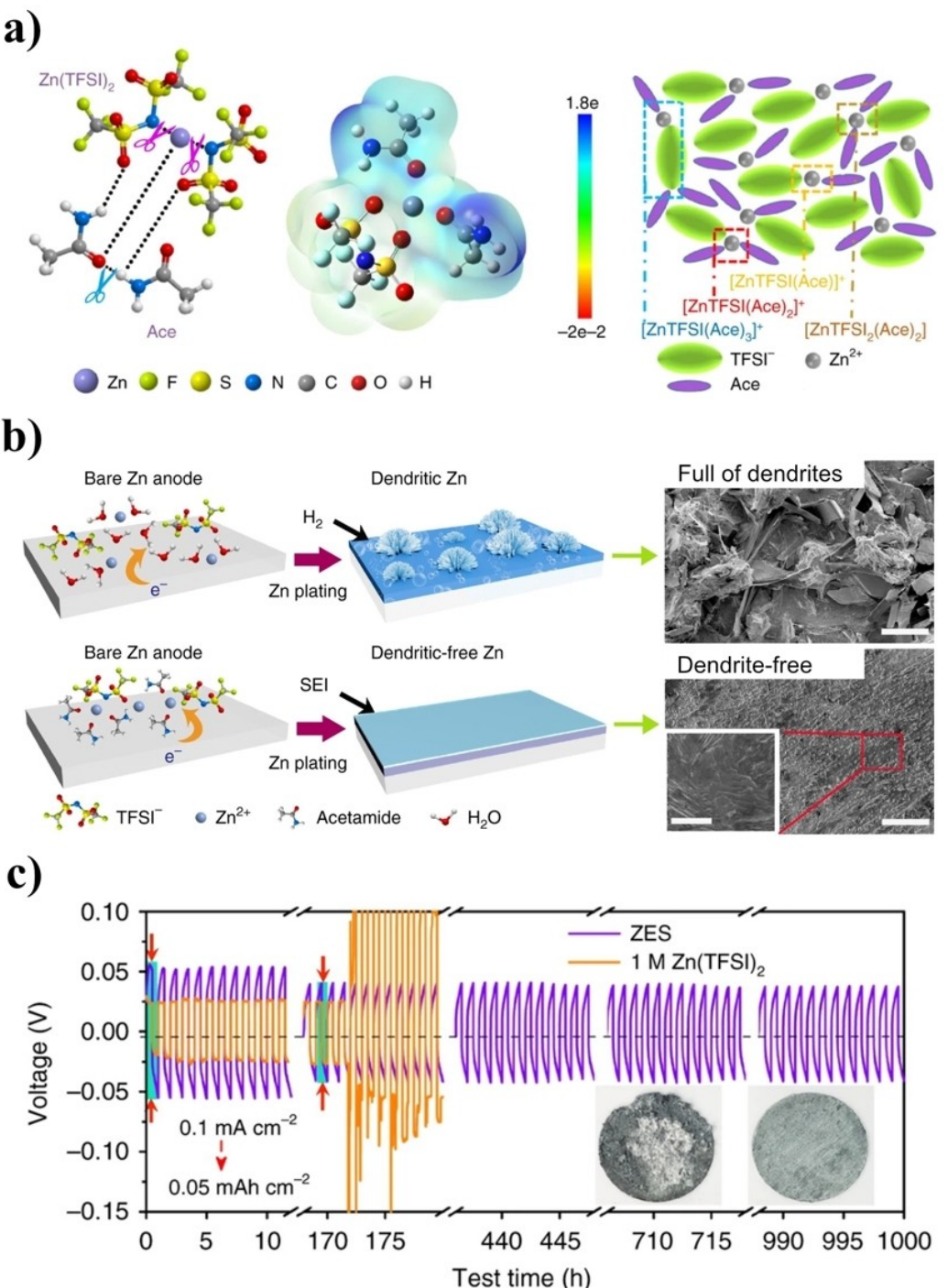


Figure 9. a) Schema of the solvated structure of $\text{Zn}(\text{TFSI})_2$ and Ace within ZES obtained based on DFT calculation. b) Schema of the comparison between water-based electrolyte [1 M $\text{Zn}(\text{TFSI})_2$] and ZES upon Zn deposition, and SEM images of the obtained Zn (0.5 mAh/cm², 1.0 mA/cm²). c) GCD cycling results of Zn/Zn cell having ZES electrolyte.^[31b] Reproduced from Ref. [31b]. Copyright (2019) The Author(s).

3.2.5. Other eutectic solvent electrolytes

As reported by Zhao et al. (2019),^[37] Zn plating/stripping can also be made via LiTFSI:urea DES electrolyte having $\text{Zn}(\text{TFSI})_2$. In this research, the fraction of LiTFSI, $\text{Zn}(\text{TFSI})_2$, urea and water was optimized to achieve the best electrochemical properties. The 1:0.05:3.8:2.0 of LiTFSI: $\text{Zn}(\text{TFSI})_2$:urea:water by mole, called LZ-DES/ $2\text{H}_2\text{O}$, was found to

be highly ion-conductive (1.85 mS/cm at 30 °C) and electrochemically stable (above 2.2 V vs. Zn/Zn^{2+} of anodic limit, Figure 10a). Via LZ-DES/ $2\text{H}_2\text{O}$ electrolyte, the SS/Zn cell displayed 96.2% of CE upon the GCD test at 0.5 mA/cm² of current density. Over 2,400 h total time of GCD test (0.1 mA/cm² of current density and 0.74 h of charge/discharge time) was passed using Zn/Zn cell and LZ-DES/ $2\text{H}_2\text{O}$ electrolyte (Fig-

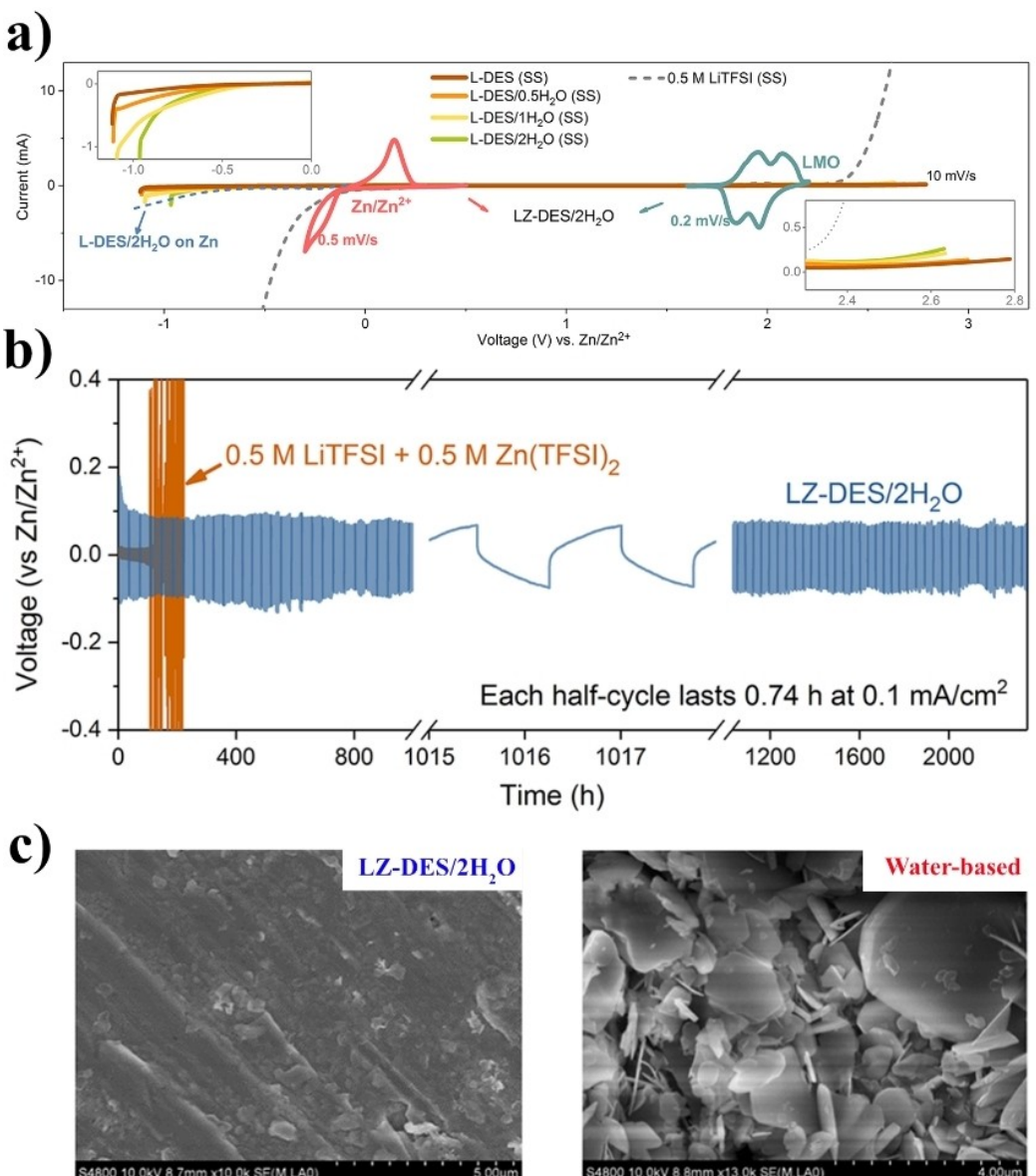


Figure 10. a) Electrochemical stability window of LZ-DES/2H₂O in comparison with other electrolytes and the operating window of $Zn/LiMn_2O_4$. b) GCD cycling results of Zn/Zn cell having LZ-DES/2H₂O electrolyte. c) Cycled Zn anode (LZ-DES/2H₂O vs. 0.5 M Li(TFSI)₂/0.5 M Zn (TFSI)₂-water).^[37] Reproduced with permission from Ref. [37]. Copyright (2018) Wiley-VCH.

ure 10b). In addition, the Zn anode after cycling was found to be dendrite-free (Figure 10c).

3.3. NAQ-GPEs

Most of the NAQ-GPE research (Table 3) focused mainly on the characterization of the produced GPE. The Zn/GPE/Zn cells were characterized using multiple cycle CV in these studies. The primary purpose of such an experiment was to evaluate the stability of the GPE. Unfortunately, there are very little data regarding Zn plating/stripping achieved from these works, and there is no further implementation after the proposition up to now. Hence, this is the gap that requires further investigation.

One of the systems among NAQ-GPEs that provide clear evidence of the Zn anode test was reported by Ma et al.^[13] The GPE was fabricated from PVDF-HFP matrix having 5% PEO and the $Zn(BF_4)_2$ -[C₂mim]BF₄ liquid electrolyte. The PEO addition results in the improved flexibility and modulus of the GPE. This combination achieved high ionic conductivity (16.9 mS/cm). Upon the GCD test using Zn/Zn cell at the testing capacity of 0.5 mAh/cm² and current of 0.2 mA/cm², the cell displays the stable operation up to 1000 h. Furthermore, it provides a dense and smooth Zn surface after cycling. In addition, there is only a negligible difference in the Zn plating efficiency of IL-GPE (99.32%) and pure IL (99.36%) sample.

4. Cathode Material for NZIBs

4.1. Manganese-based cathodes

4.1.1. Manganese dioxide (MnO_2)

In the development of ZIBs, MnO_2 , which possesses high specific capacity and rechargeability, is one of the most studied host materials. The specific capacity of MnO_2 is 616 mAh/g; calculation is based on two-electron redox reactions i.e., Mn (IV) to Mn (II).^[73] However, it is noted that research undertaken cannot get close to such a theoretical value.^[3,74] In general, Zn/ MnO_2 batteries, having aqueous electrolytes i.e., aqueous $ZnSO_4$, aqueous $ZnCl_2$, aqueous $Zn(OTf)_2$ and other aqueous electrolytes, exhibit >200 mAh/g of specific capacity and ~ 1.3 V of average voltage, which is high enough for practical application.^[2,74]

Different phases of MnO_2 (α -, β -, γ -, and δ -, Figure 11a) and different nanostructure shapes provide quite different characteristics and unequal performance.^[75] For example, it is seen that the 2×2 tunnels host such as α - MnO_2 and the aqueous $ZnSO_4$ electrolyte, two reactions viz. intercalation of Zn^{2+} and intercalation of H^+ are involved in the charge-storage mechanism, while there is only the intercalation of Zn^{2+} when the layered-type δ - MnO_2 is used as host material.^[3] In addition, other factors e.g., Zn salt choices as well as supporting electrolyte additives play an important role in determining the performance of the MnO_2 cathode.^[2]

Most MnO_2 based ZIB research have been conducted using aqueous electrolytes. Yet, since the severe H_2 production issue in aqueous systems was revealed, attempts have been made to use nonaqueous electrolytes instead. In fact, Venkata Narayanan et al. (2010)^[36] first reported the NZIB based on the MnO_2 cathode. The γ - MnO_2 having $Zn(ClO_4)_2$:Acetone DES electrolyte yielded a first discharge capacity of 190 mAh/g and the stabilized discharge capacity (after 10 cycles passed) of 90 mAh/g (Figure 11b). A trace of Zn in the discharged γ - MnO_2 cathode was revealed using the EDAX technique (Figure 11c), thus indicating that the Zn intercalation into the γ - MnO_2 is the main charge-storage reaction within the $Zn(ClO_4)_2$:Acetone/ γ - MnO_2 system. Furthermore, there are some reports suggesting GPEs containing imidazolium ionic liquid for the Zn/ MnO_2 batteries.^[40,44,45] The capacity of these systems is in the range of 120–125 mAh/g.

Han et al. (2017)^[18d] investigated the intercalation mechanism of Zn into δ - MnO_2 within $Zn(TFSI)_2$ -AN electrolyte. In the study, it is seen that the source of δ - MnO_2 cathode capacity in $Zn(TFSI)_2$ -AN arose from the ~ 0.6 oxidation change of Mn atom (from 3.8+ at charged state to 3.2+ at discharged state). It was also found that there was no significant structural or phase transformation of δ - MnO_2 cathode upon the Zn^{2+} insertion; the only change noticed was the change in the unit cell volume. Thus, the intercalation reaction within AN electrolyte could be more reversible than that of an aqueous system, which has the spinel $ZnMn_2O_4$ as a main discharge product (δ - $MnO_2 \leftrightarrow$ spinel $ZnMn_2O_4$). However, only 123 mAh/g of maximum discharge capacity (at 12.3 mA/g), poor rate capability and low voltage

(more than a half of discharge profile < 1 V, Figure 11d) were achieved from the Zn/ δ - MnO_2 cell having $Zn(TFSI)_2$ -AN electrolyte. In addition, electrochemical characterization results revealed the formation of a passivation layer on the cathode upon cycling, which led to poor capacity retention. As reported by Kao-ian et al. (2021),^[9] the Zn/ δ - MnO_2 cell having $Zn(OTf)_2$ -DMSO electrolyte attained higher performance (1.15 V of nominal voltage and 159 mAh/g of specific capacity at 50 mA/g, Figure 11e) and cyclability (1,000 cycles, 60% capacity retention, Figure 11f). Corpuz et al. (2020)^[22] recorded the use of α - MnO_2 in NZIB. Thus, it was found that Zn/ α - MnO_2 having $Zn(OTf)_2$ -DMSO exhibited only 60 mAh/g of specific capacity at 100 mA/g, but, in terms of stability, this battery can cycle up to 2,000 cycles.

4.1.2. $LiMn_2O_4$ spinel

Another manganese oxide host used in Zn batteries using nonaqueous media is the cubic spinel $LiMn_2O_4$ (Figure 12a). $LiMn_2O_4$ allows reversible Li^+ intercalation within a range of $1 \leq x \leq 2$ ($Li_xMn_2O_4$) yielding a theoretical capacity of 148 mAh/g.^[77] Within this range, $LiMn_2O_4$ can maintain its cubic structure, and there is only 6.5% of volume change found at full-intercalation (discharged). The application of $LiMn_2O_4$ in a Zn battery can be made using a Zn^{2+}/Li^+ contained electrolyte. Upon the battery discharging, Li^+ is intercalated at the cathode whereas Zn is stripped from the anode.^[37] Consequently, the Zn/ $LiMn_2O_4$ cell having LZ-DES/2H₂O electrolyte delivered 117 mAh/g of initial capacity (0.06 C) and ~ 1.92 V discharge voltage (Figure 12b). The cell retained 70% capacity at a higher rate (1 C). Upon the cyclability test, 82.7% capacity retention was achieved after 600 cycles (Figure 12c). In this system, the high content of water (~ 30 mol%) of LZ-DES/2H₂O may be the source of the facile Li^+ intercalation kinetics.^[78] However, it is noted that the Zn/ $LiMn_2O_4$ system cannot run perfectly under the aqueous electrolyte: this is due to the high terminal charging voltage of the Zn/ $LiMn_2O_4$ cell (> 2 V), which is higher than the stability limit of the aqueous electrolyte (~ 2 V, Figure 12d).

4.2. Vanadium-based cathodes

4.2.1. Vanadium oxide

Due to their large-inter spacing and high specific capacity, vanadium oxides i.e., V_2O_5 , $V_2O_5 \cdot nH_2O$, $V_3O_7 \cdot H_2O$ and XV_2O_5 , where X=Zn, Na, Ca..., which are constructed from the VO_5 pyramid or the VO_6 octahedra, are attractive host material for ZIBs.^[2,80] According to the literature, the Zn^{2+} intercalation capacities of vanadium oxides in aqueous media range from 224 to 470 mAh/g, and originate from the V^{5+} to V^{4+} or even to V^{3+} of the oxidation state changes of vanadium atoms.^[81] Several reports state that most of the vanadium oxide cathodes provide exceptional rate capability: this is due to the large inter-space of the vanadium oxides, which can further be enhanced by adding water molecules or cations into their

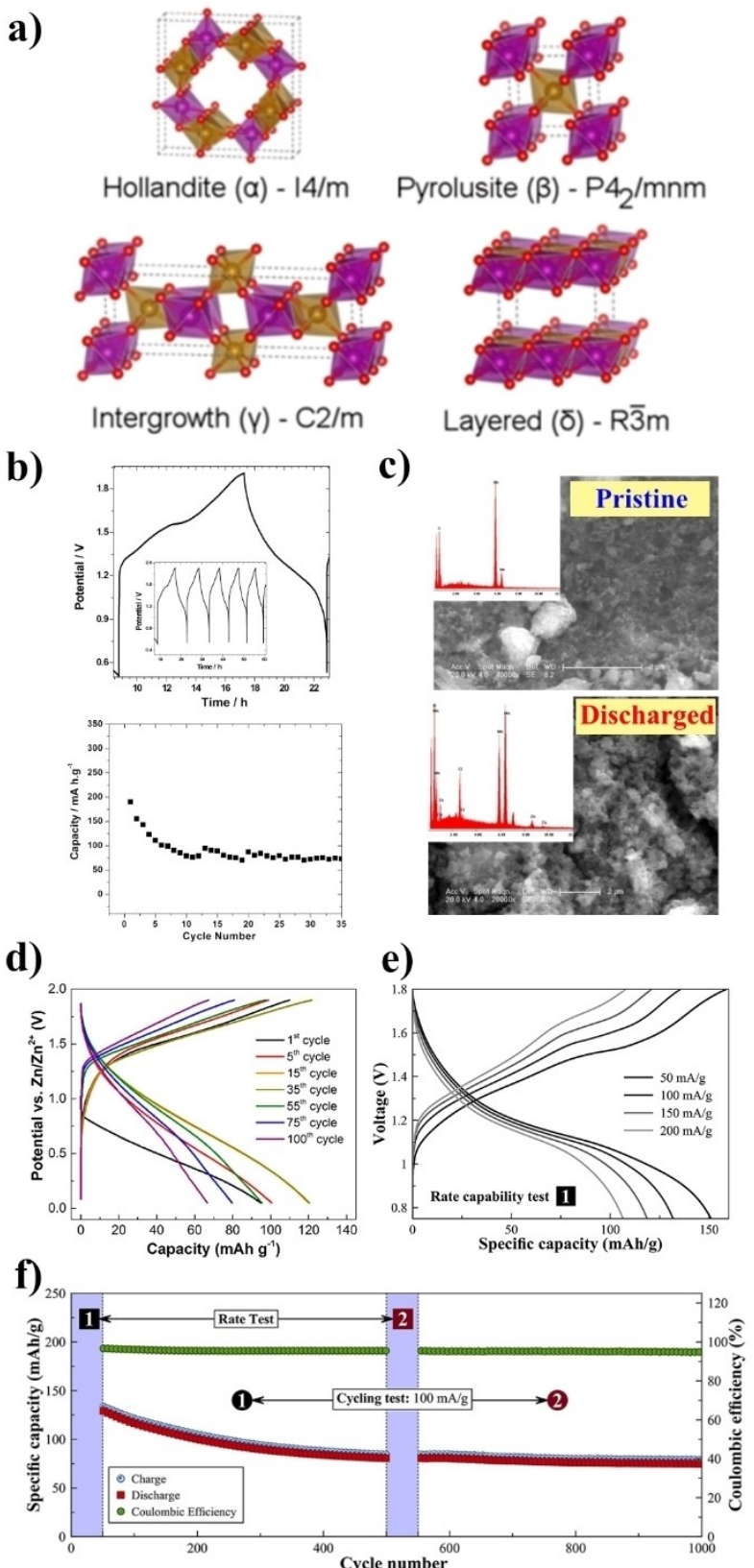


Figure 11. a) Schema of the crystal structure of α -, β -, γ -, and δ - MnO_2 .^[76] Reproduced from Ref. [76]. Copyright (2016) The Author(s). Published by the American Physical Society. b) GCD cycling results of $\text{Zn}/\gamma\text{-MnO}_2$ having $\text{Zn}(\text{ClO}_4)_2\text{:Ac}$ DES electrolyte ($100 \mu\text{A/cm}^2$, MnO_2 loading: 4.5 mg/cm^2). c) SEM images (EDAX included) of pristine and discharged electrodes.^[36] Reproduced with permission from Ref. [36]. Copyright (2009) Elsevier Inc. d) GCD cycling results of $\text{Zn}/\delta\text{-MnO}_2$ having $0.5 \text{ M Zn}(\text{TFSI})_2\text{:AN}$ electrolyte at 12.3 mA/g .^[18d] Reproduced with permission from Ref. [18d]. Copyright (2017) American Chemical Society. e and f) GCD cycling results of $\text{Zn}/\delta\text{-MnO}_2$ having $0.25 \text{ M Zn}(\text{OTf})_2\text{:DMSO}$ electrolyte.^[9] Reproduced from Ref. [9]. Copyright (2021) The Author(s). Published by Elsevier Ltd.

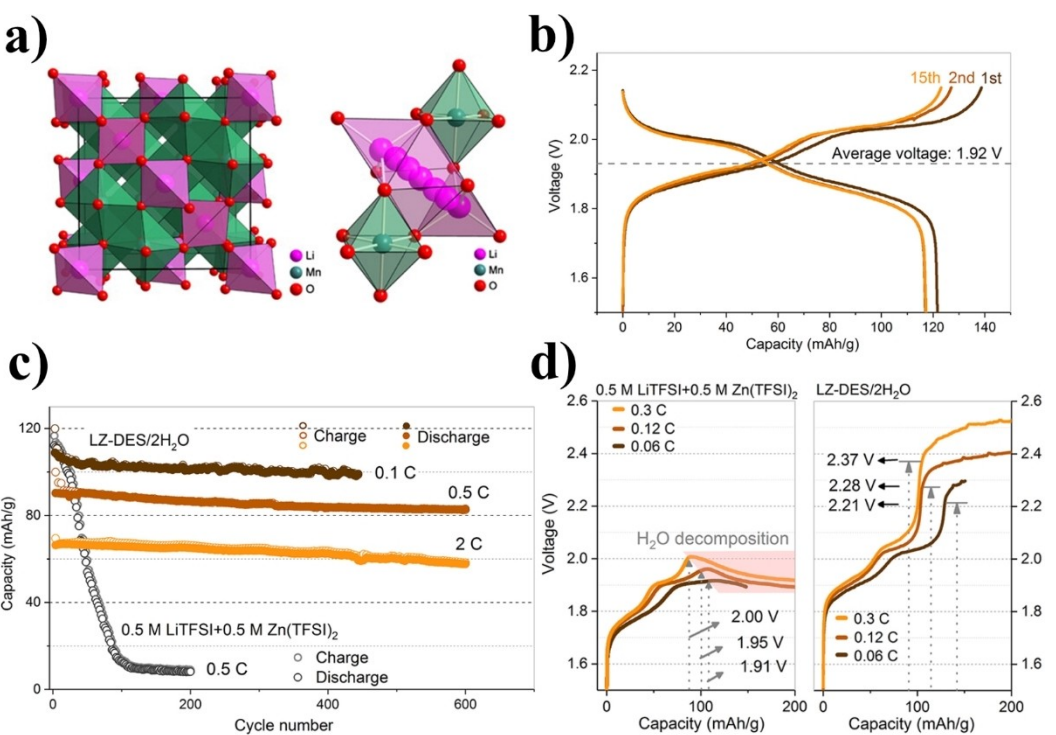


Figure 12. a) Crystal structure of LiMn_2O_4 .^[79] Reproduced from Ref. [79]. Copyright (2013) Chinese Materials Research Society. Production and hosting by Elsevier B.V. b) GCD discharge profile of $\text{Zn}/\text{LiMn}_2\text{O}_4$ cell ($\text{LZ-DES}/2\text{H}_2\text{O}$) during first few cycles. c) GCD cycling performance of $\text{Zn}/\text{LiMn}_2\text{O}_4$ cell at various current rate. d) Charging limits of $\text{Zn}/\text{LiMn}_2\text{O}_4$ cell having water-based (left) and $\text{LZ-DES}/2\text{H}_2\text{O}$ (right) electrolyte.^[37] Reproduced with permission from Ref. [37]. Copyright (2018) Elsevier Ltd.

layers.^[3] However, the main disadvantage of vanadium oxides is the low discharge voltage ($\sim 0.8\text{--}1\text{ V}$). As for the nonaqueous media, vanadium oxides are found to be compatible with $\text{Zn}(\text{TFSI})_2\text{-AN}$, $\text{Zn}(\text{OTf})_2$ and ZES.^[18b,f,31b]

Senguttuvan et al. (2016)^[18f] stated that an average voltage of 0.85 V on a specific capacity of 170 mAh/g was achieved from a $\text{Zn}/\text{V}_2\text{O}_5$ cell having $\text{Zn}(\text{TFSI})_2\text{-AN}$ electrolyte. It is noted that the cell exhibited excellent rate capability and was able to cycle at least 120 cycles with negligible capacity loss (Figure 13a). Qiu et al. (2019)^[31b] proposed the use of ZES as an electrolyte for a $\text{Zn}/\text{V}_2\text{O}_5$ cell. Accordingly, it was found that $\sim 150\text{ mAh/g}$ capacity (80 mA/g), $\sim 0.9\text{ V}$ discharge voltage (80 mA/g) and 92.8% capacity retention after 800 cycles (at 600 mA/g) were achieved (Figure 13b and c). It is significant that all the $\text{Zn}/\text{V}_2\text{O}_5$ cells conducted in the nonaqueous media provided lower capacity than in the aqueous electrolyte. Kundu et al. (2018)^[18b] reported on the phenomena behind such outcomes. In Kundu's study, it was seen that a similar charge-storage mechanism between aqueous and nonaqueous systems was found (according to the XRD and XPS analysis) whereby the $\text{V}_3\text{O}_7\text{-H}_2\text{O}$ cathode provided 375 mAh/g at 1 C and 275 mAh/g at 8 C in the aqueous ZnSO_4 electrolyte; such a good performance, however, was not afforded by $\text{Zn}(\text{OTf})_2\text{-AN}$ ($\sim 59\text{ mAh/g}$ at 5 mA/g). It was found that desolvation was the main process that determined the rate performance of the battery: the desolvation energy required in nonaqueous systems is much higher than that in aqueous systems. Thus, the

performance of the nonaqueous battery was tremendously reduced.

4.2.2. Vanadium sulfide

It is found that reversible Zn^{2+} intercalation can be made using layered vanadium sulfide (VS_2). He et al. (2017)^[82] stated that via the $\text{V}^{4+}/\text{V}^{3+}$ oxidation change, the Zn/VS_2 having an aqueous ZnSO_4 electrolyte can provide 190.3 mAh/g of specific capacity (50 mA/g) and $\sim 0.6\text{ V}$ discharge voltage. Further, according to Naveed et al. (2019), Zn/VS_2 can run under TMP-DMC electrolyte achieving 94.38% capacity retention after 500 cycles.^[21] However, both low capacity (maximum 146.6 mAh/g) and the low voltage ($\sim 0.45\text{ V}$) were recorded.

4.2.3. Vanadium-based polyanionic compounds

Another state-of-art of the vanadium-based electrode is the polyanionic compound. Li et al. (2016)^[83] introduced polyanionic cathodes having NASICON structure such as $\text{Na}_3\text{V}_2(\text{PO}_4)_3$ (NPV) for use in ZIBs. The NASICON structure of NPV allows fast Na^+ diffusion and further results in fast intercalation kinetics. The study also reported that the first charging resulted in Na^+ extraction from the NPV (V^{3+}), thus forming $\text{NaV}_2(\text{PO}_4)_3(\text{V}^{4+})$. Subsequently, Zn^{2+} intercalation/deintercalation took place. Thus, the Zn/NPV cell having aqueous $\text{Zn}(\text{CH}_3\text{COO})_2$ electrolyte

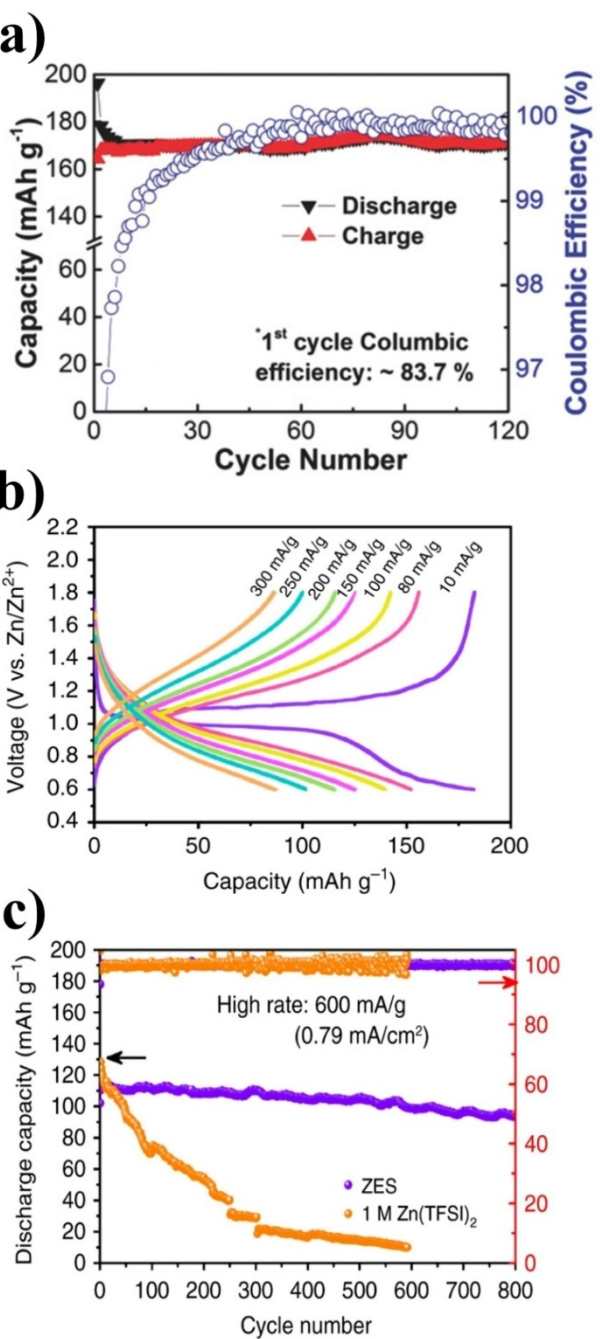


Figure 13. Electrochemical performance of nonaqueous $\text{Zn}/\text{V}_2\text{O}_5$ batteries: a) GCD cycling results of $\text{Zn}/\text{V}_2\text{O}_5$ cell having 0.5 $\text{Zn}(\text{TFSI})_2\text{-AN}$ at C/10 (14.4 mA g^{-1}).^[18f] Reproduced with permission from Ref. [18f]. Copyright (2016) Wiley-VCH. b) GCD voltage profile of $\text{Zn}/\text{V}_2\text{O}_5$ cell having ZES electrolyte at various current densities (10–300 mA g^{-1}). c) Cyclability results of $\text{Zn}/\text{V}_2\text{O}_5$ cell having ZES at 600 mA g^{-1} (ZES vs. aqueous).^[31b] Reproduced from Ref. [31b]. Copyright (2019) The Author(s).

provided 97 mAh g^{-1} specific capacity (0.5 C) and ~1.1 V discharge voltage. Guo et al. (2017)^[84] next surveyed the development of polyanionic cathodes. It is noted that O^{2-} and F^- had high electronegativity, which was able to enhance the voltage of the cathode. Consequently, a $\text{Na}_3\text{V}_2(\text{PO}_4)_2\text{O}_2\text{F}$ (NVPOF) cathode was introduced for use in a Na-ion battery. Dong et al. (2020)^[16d] put forward the use of NVPOF in ZIBs. Consequently,

having 0.5 M/1.0 M of $\text{Zn}(\text{OTf})_2/\text{NaClO}_4\text{-TMP}$ electrolyte, the Zn/NVPOF cell (Figure 14a) provided a high specific capacity of 113 mAh g^{-1} and an average discharge voltage of 1.8 V (Figure 14b). In addition, 83.5% capacity retention was achieved upon 1,000 cycles (Figure 14c). The charging voltage cut-off of this battery was 2.2 V; thus, the use of the aqueous electrolyte proved infeasible. Different from what it was in the aqueous Zn/NPV system, Na^+ intercalation took place in the Zn/NVPOF having 0.5 M/1.0 M of $\text{Zn}(\text{OTf})_2/\text{NaClO}_4\text{-TMP}$ electrolyte instead of Zn^{2+} intercalation: this may be the cause of the improved stability of the Zn/NVPOF system.

Another polyanionic cathode found in nonaqueous Zn battery research is the layered VOPO₄, which was further enhanced by adding a preintercalated polypyrrole (PPy) into VOPO₄ interspace.^[18c] The PPy addition was found to reduce the interspacing size and improved the electronic conductivity of VOPO₄. The $\text{Zn}/\text{PPy-VOPO}_4$ cell having water, containing $\text{Zn}(\text{OTf})_2\text{-AN}$ electrolyte exhibited 1.1 V average voltage and maximum capacity of 86 mAh g^{-1} . Besides, the cell passed at least 350 cycles at a current density of 100 mA g^{-1} .

4.3. Cobalt based cathodes

The cobalt oxide e.g., LiCoO_2 is a traditional host material, which has been used in LIBs for more than a decade.^[85] The intercalation fraction (x) of Li^+ to Li_xCoO_2 ranges from $x=0$ (Co^{4+}) to $x=1$ (Co^{3+}) having 274 mAh g^{-1} theoretical capacity. Due to their large capacity, 3D-tunnel structure and high voltage, attempts have been made to apply the CoO_2 framework to ZIBs. Pan et al. (2017)^[16b] first proposed the use of CoO_2 framework (ZnCo_2O_4 form) in ZIBs. To compensate for the instability issue of the spinel ZnCo_2O_4 caused by oxygen evolution, Al was doped in ZnCo_2O_4 to form the more stable $\text{ZnAl}_x\text{Co}_{2-x}\text{O}_4$ (Figure 15a). Material characterizations highlight the fact that there was a reversible change in the Co oxidation state upon discharging/charging ($\text{Co}^{4+} \leftrightarrow \text{Co}^{3+}$). CV results revealed that the best electrochemical performance was achieved at $x=0.67$ ($\text{ZnAl}_{0.67}\text{Co}_{1.33}\text{O}_4$). The $\text{Zn}/\text{ZnAl}_{0.67}\text{Co}_{1.33}\text{O}_4$ cell having $\text{Zn}(\text{OTf})_2\text{-AN}$ electrolyte provided 134 mAh g^{-1} (~84% of theoretical capacity) of initial discharge capacity and ~1.7 V discharge voltage at 0.1 C (16 mA g^{-1}) (Figure 15b). At 1 C, capacity retained only 70% of its initial capacity (Figure 15c); this outcome indicates the limitation of this system in terms of rate capability.

The CoO_2 framework for ZIBs was further developed by the same group work. Pan et al. (2018)^[16c] noted that the inadequate Zn^{2+} diffusion rate was the cause of the deficient performance of the Al-doped ZnCo_2O_4 cathode; it was found that Zn^{2+} in the cathode was not fully extracted during the charging process. To improve capacity and structural stability, $\text{ZnNi}_x\text{Mn}_x\text{Co}_{2-2x}\text{O}_4$, containing Ni and Mn, was introduced. According to the GCD test, the optimized formula of $\text{ZnNi}_x\text{Mn}_x\text{Co}_{2-2x}\text{O}_4$ was found to be $\text{ZnNi}_{1/2}\text{Mn}_{1/2}\text{CoO}_4$. The $\text{Zn}/\text{ZnNi}_{1/2}\text{Mn}_{1/2}\text{CoO}_4$ cell having $\text{Zn}(\text{OTf})_2\text{-AN}$ electrolyte possessed a high capacity of 180 mAh g^{-1} (0.1 C ≈ 21 mA g^{-1}) and provided excellent cyclability (>200 cycles at 0.2 C) (Figure 15e). The

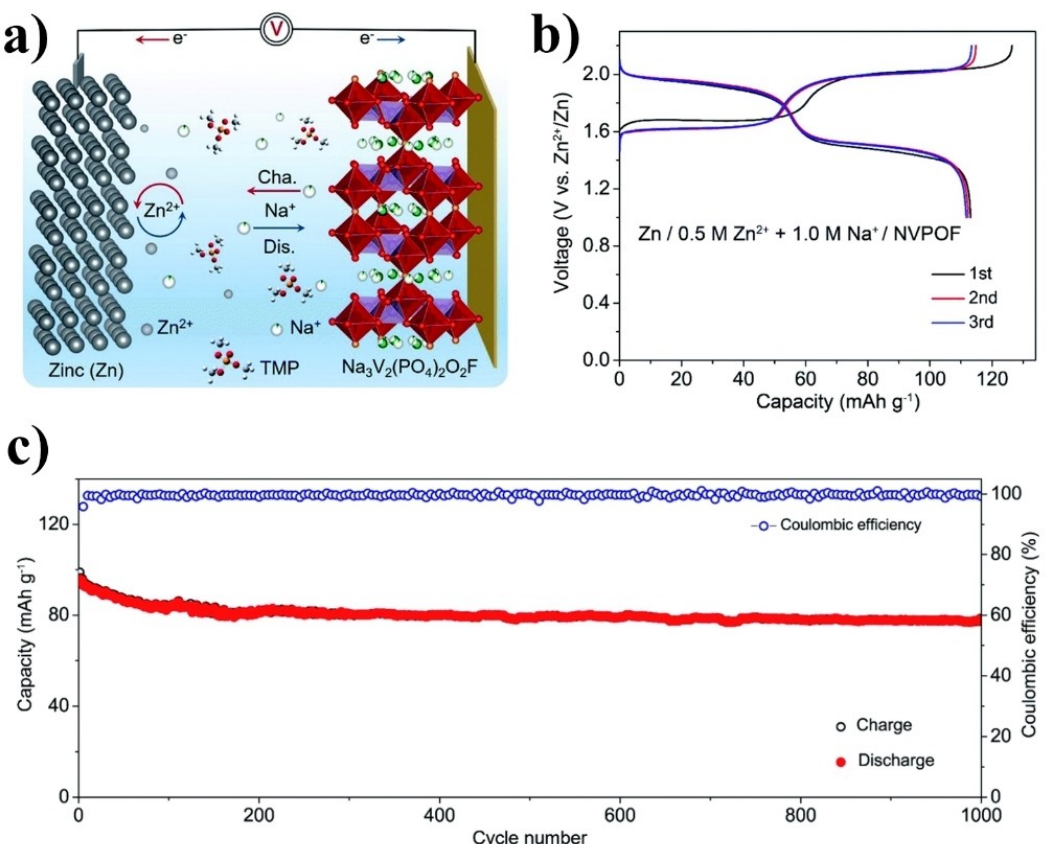


Figure 14. a) Schema of the Zn/NVPOF dual-ion battery. b) GCD discharge profiles of Zn/NVPOF cell having 0.5 M/1.0 M of $\text{Zn}(\text{OTf})_2/\text{NaClO}_4$ -TMP electrolyte at 0.2 C. c) GCD cycling results of Zn/NVPOF cell at 1.0 C. ^[16d] Reproduced with permission from Ref. [16d]. Copyright (2020) The Royal Society of Chemistry.

enhanced capacity arose from the additional redox sources i.e., $\text{Mn}^{4+}/\text{Mn}^{3+}$ and $\text{Ni}^{4+}/\text{Ni}^{3+}/\text{Ni}^{2+}$ (Figure 15d) instead of only $\text{Co}^{4+}/\text{Co}^{3+}$ as in the case of $\text{ZnAl}_x\text{Co}_{2-x}\text{O}_4$. Besides, there was an improved rate capability compared to the $\text{ZnAl}_x\text{Co}_{2-x}\text{O}_4$; at 1 C the capacity retained 80% of its initial capacity (Figure 15f).

4.4. Prussian blue-based cathodes

Prussian blue analogue (PBA) is a high voltage host material, which is constructed following the $M\text{Fe}(\text{CN})_6$ formula where $M=\text{Zn, Cu, Ni, Mn, Co}$ and other transition metals, $M\text{HCf}$.^[3] PBAs always appear in cubic or monoclinic forms. Nonaqueous electrolytes are required for the ZIBs having PBA cathodes to avoid electrolyte decomposition upon charging. The specific capacity of PBA in nonaqueous media ranges from 50 to 190 mAh/g, depending on the type of M species. Munseok et al. (2017) reported the use of KNIHCf having the formula $K_{0.86}\text{Ni}[\text{Fe}(\text{CN})_6]_{0.954}(\text{H}_2\text{O})_{0.766}$ as cathode material for NZIB.^[18e] Via $\text{Zn}(\text{ClO}_4)_2\text{-AN}$ electrolyte, Zn/KNIHCf cell exhibited a first discharge capacity of 55.6 mAh/g (0.2 C \approx 11.2 mA/g), which is about 67% of the theoretical capacity. XRD and EDX results confirmed the insertion/extraction of Zn^{2+} (Figure 16a). However, poor rate capability was noted; capacity decreased progressively as the current increased (Figure 16b).

Naveed et al. (2019)^[16a] set up $\text{KCuFe}(\text{CN})_6$ (KCuHCf) for use in a NZIB. In the $\text{Zn}(\text{OTf})_2\text{-TEP}$ electrolyte, the Zn/KCuHCf cell failed at cycling; capacity decreased progressively during the first 5 cycles. It is evident that water should have been added to the electrolyte to drive the Zn^{2+} intercalation. The Zn/KCuHCf having $\text{Zn}(\text{OTf})_2\text{-TEP:water}$ (7:3 by volume) electrolyte passed 1,000 cycles of GCD test at 1 C (\sim 73.3 mA/g), yielding 74% capacity retention (Figure 16c). The cell provided 73.3 mAh/g of initial capacity and \sim 1.6 V of discharge voltage at 0.5 C. In addition, superior rate performance was obtained; a slight decrease in capacity occurred when the cell cycled at 0.5 C to 2 C (Figure 16d).

As presented by Li et al. (2020),^[15b] the $K_{1.6}\text{Mn}_{1.2}\text{Fe}(\text{CN})_6$ (KMnHCf) cathode is viewed as one of the most promising cathodes for NZIBs displaying a reversible change between cubic monoclinic (discharge) and (charged) structure upon Zn^{2+} interaction/deintercalation. Thus, the Zn/KMnHCf in $\text{Zn}(\text{ClO}_4)_2\text{-TEGDME}$ exhibited a high discharge voltage (1.6 V), a high specific capacity (65.5 mAh/g at 50 mA/g), a good rate capability (65, 52, 48, and 45 mAh/g capacity at 50 to 100, 150 and 200 mA/g current density, respectively) and excellent cyclability [94% capacity retention at 8,500 cycles (200 mA/g)]. The cell also revealed negligible self-discharge (3% capacity loss) upon one week rest period (Figure 16e).

Another PBA cathode found in NZIB research is CoHCf .^[13] According to Ma et al. (2020), a CoHCf nanocube cathode,

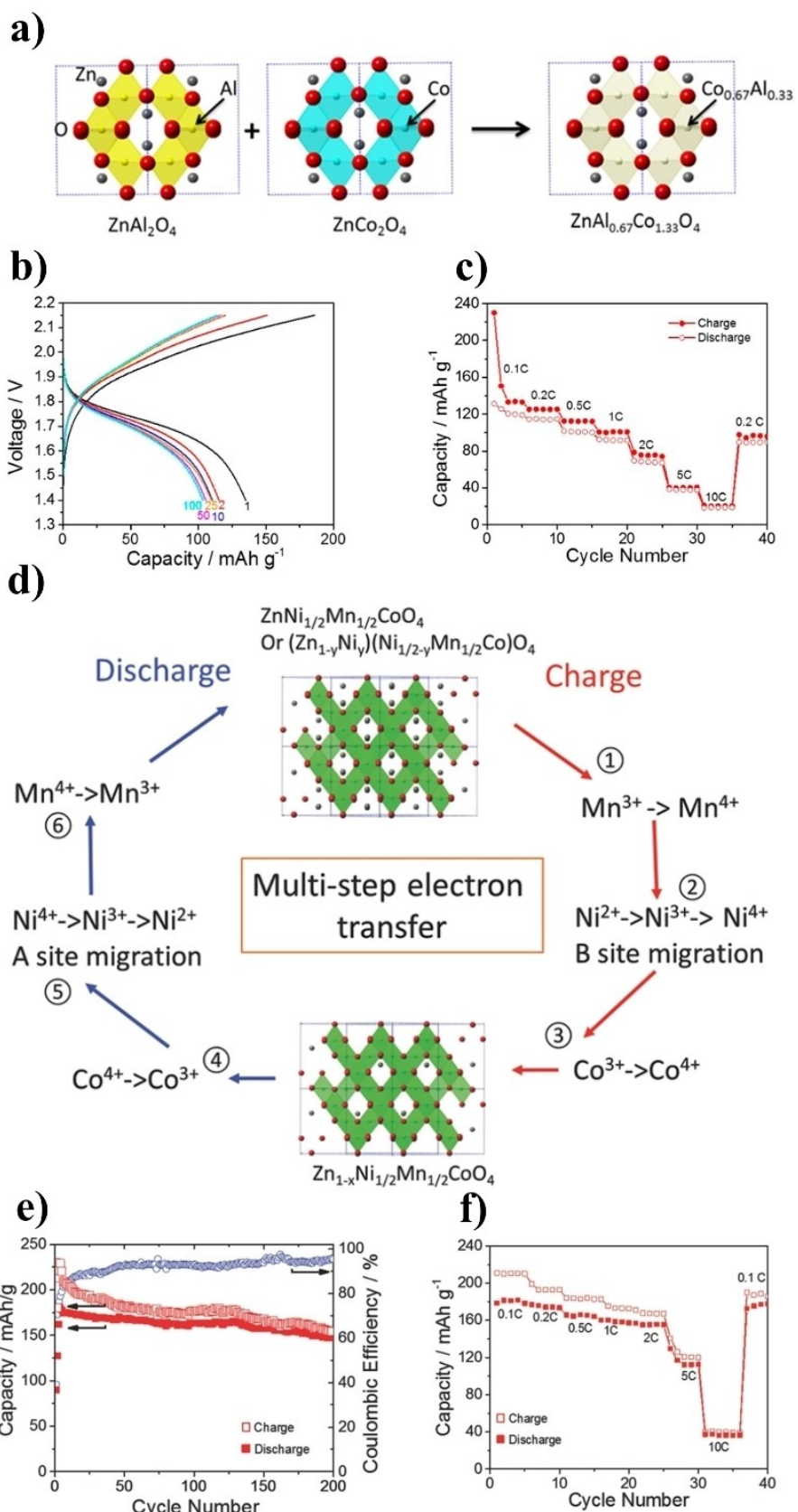


Figure 15. a) Schema of the crystal structure of $\text{ZnAl}_{0.67}\text{Co}_{1.33}\text{O}_4$. b) GCD discharge (0.2 C) profile of $\text{Zn/ZnAl}_{0.67}\text{Co}_{1.33}\text{O}_4$ cell ($\text{Zn}(\text{OTf})_2\text{-AN}$ electrolyte) at various cycling position. c) Rate capability results of $\text{Zn/ZnAl}_{0.67}\text{Co}_{1.33}\text{O}_4$ cell.^[16b] Reproduced with permission from Ref. [16b]. Copyright (2017) American Chemical Society. d) Schema of charge-charge storage reactions of $\text{ZnNi}_x\text{Mn}_x\text{Co}_{2-x}\text{O}_4$ cathode. e) Cyclability results of $\text{Zn/ZnNi}_x\text{Mn}_x\text{Co}_{2-x}\text{O}_4$ cell ($\text{Zn}(\text{OTf})_2\text{-AN}$ electrolyte) at 0.2 C. f) Rate capability results of $\text{Zn/ZnNi}_x\text{Mn}_x\text{Co}_{2-x}\text{O}_4$ cell.^[16c] Reproduced with permission from Ref. [16c]. Copyright (2018) Wiley-VCH.

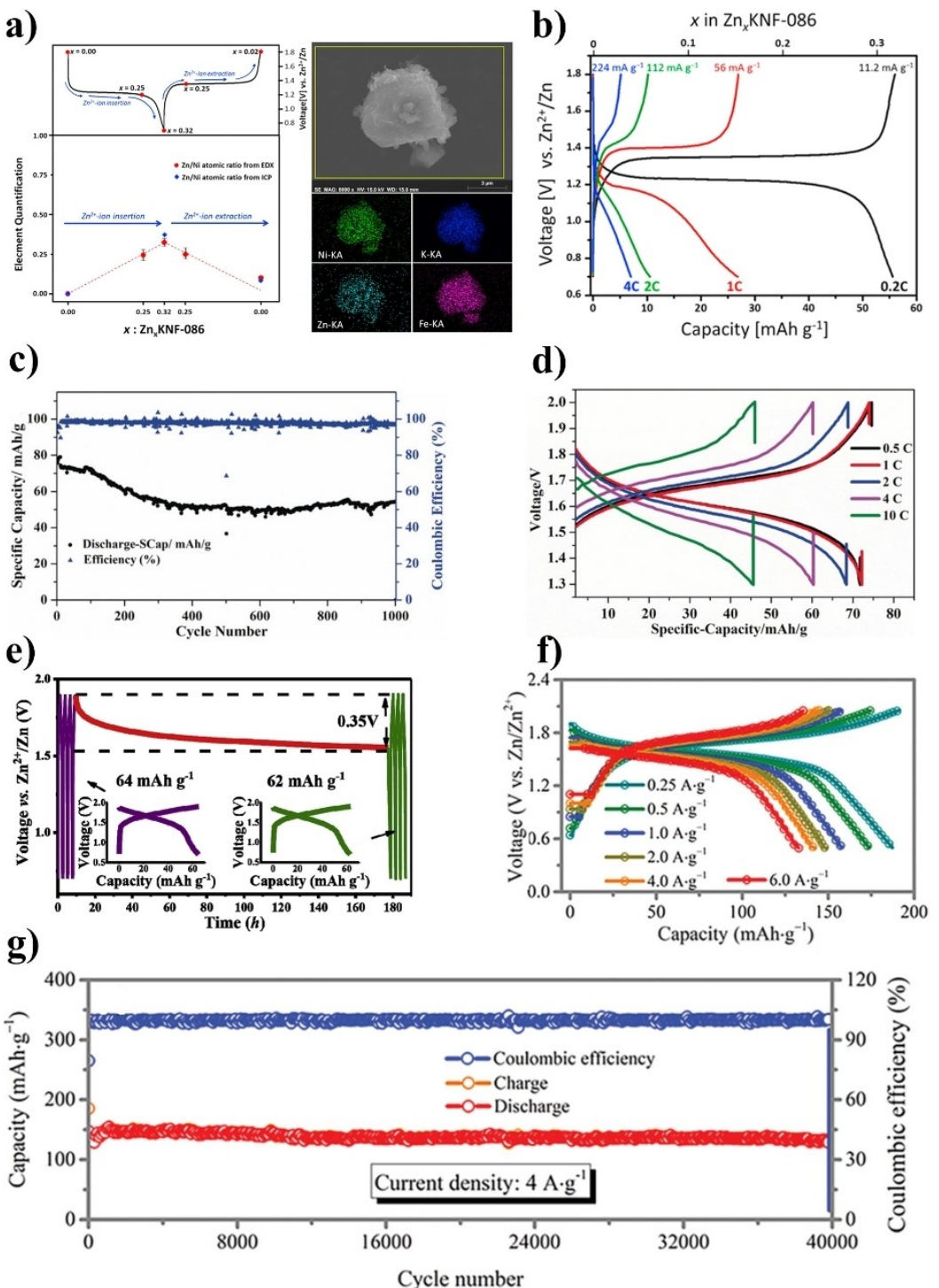


Figure 16. a and b) Zn/KNiHcf system ($\text{Zn}(\text{ClO}_4)_2\text{-AN}$): a) voltage vs. intercalation fraction (left) and SEM-EDX image of discharged cathode (right). b) Rate capability results of Zn/KNiHcf cell.^[18e] Reproduced with permission from Ref. [18e]. Copyright (2017) Elsevier. c and d) Zn/KCuHcf system ($\text{Zn}(\text{OTf})_2\text{-TEP:water}$): c) cyclability result of Zn/KCuHcf cell at 1 C, d) rate capability results of Zn/KCuHcf cell.^[16a] Reproduced with permission from Ref. [16a]. Copyright (2019) Wiley-VCH. e) Self-discharge test of Zn/KMnHcf cell ($\text{Zn}(\text{ClO}_4)_2\text{-TEGDME}$).^[15b] Reproduced with permission from Ref [15b]. Copyright (2020) Elsevier. f and g) Zn/CoHcf system ($\text{Zn}(\text{BF}_4)_2\text{-[C2mim]BF}_4$): f) Rate capability results of Zn/CoHcf cell, g) cyclability results of Zn/CoHcf cell at 4 A/g.^[13] Reproduced with permission from Ref. [13]. Copyright (2020) Wiley-VCH.

having $\text{Zn}(\text{BF}_4)_2\text{-[C2mim]BF}_4$ electrolyte, delivered an extremely high capacity of 187.3 mAh/g at 250 mA/g current density, which is superior to all PBA cathodes that have ever been recorded in the literature. The Zn/CoHcf cell also attained a

very wide current range of operation (0.25–6 A/g) (Figure 16f); at 6 A/g, capacity still retained 135.6 mAh/g. In addition, the cell passed 40,000 cycles (2 A/g), yielding 95% capacity retention (Figure 16g). It is noted that the contribution of both

Co ($\text{Co}^{3+} \leftrightarrow \text{Co}^{2+}$) and Fe ($\text{Fe}^{3+} \leftrightarrow \text{Fe}^{2+}$) resulted in two-electron charge-storage reactions, which provided the source of the high capacity of the CoHcf cathode.

Furthermore, there is a unique approach apart from the other PBA systems. It is reported by Li et al. (2021) that suppressing Zn intercalation by adding the high fraction of K salts to form the $\text{K}^+/\text{Zn}^{2+}$ dual ion electrolyte results in the improved performance of the Zn/ZnHCF cell compared to the use of pure Zn ion electrolyte.^[20] This outcome reflects the effect of valency on the intercalation reaction. The cation with lower valency possesses more easy diffusion and faster kinetic than that of the higher valency cation. In addition, the study showed the exceptional rate capability and cyclability (74% capacity retention after 100,000 GCD cycles at a rate of 2 A/g).

4.5. Organic-based cathodes

Polyaniline (PANI), a conducting polymer, is one of the organic-based cathodes, which can be used in NZIBs. The charge-storage process of PANI relies on the reaction between anions i.e., Cl^- , TFSI^- and OTF^- and the nitrogen (imine group) on PANI molecule to form salts: upon charging, the electron on the nitrogen will be removed; accordingly, the association with anions occurs.^[86] Guerfi et al. (2014)^[19] recommended the Zn/PANI battery based on a nonaqueous electrolyte. The Zn/PANI having $\text{Zn}(\text{TFSI})_2\text{-PC}$ demonstrated maximum capacity of 148 mAh/g and an average discharge voltage of ~ 0.85 V at 0.5 C, and passed at least 1,700 cycles of GCD cycling.

A phenanthrenequinone macrocyclic trimer (PQ-MCT) is also one of the organic-based cathodes being used in NZIBs.^[15a] PQ-MCT can store Zn^{2+} on its C=O groups via coordination reaction (Figure 17a), and has a theoretical capacity of 257.74 mAh/g. Wang et al. (2020)^[15a] put forward a nonaqueous Zn/PQ-MCT battery using $\text{Zn}(\text{OTf})_2\text{-DMF}$ electrolyte. At 1 A/g, the cell was found to be extremely stable at cycling: over 20,000 cycles were achieved having negligible capacity fading (Figure 17b). The PQ-MCT cathodes exhibited 145 mAh/g of specific capacity and ~ 0.75 V vs. Zn/Zn^{2+} of average discharge voltage at 0.05 A/g. In addition, the cell was able to run at 50 A/g yielding 60 mAh/g discharging capacity (Figure 17c), and operated normally at extreme temperature conditions (-70°C and 150°C).

Another organic-based cathode for nonaqueous Zn batteries found in the literature is the polytriphenylamine composite (PTPAn).^[23] The charge-storage mechanism of PTPAn is very close to that of PANI. Upon charging, the C–N groups on PTPAn are seen to lose electrons. Then, the situation changed into the positive-charged $\text{C}=\text{N}^+$, which bonded with the guest anions i.e., TFSI^- (Figure 17d). Qiu et al. (2021)^[23] studied the application of PTPAn in NZIBs. At 2 mg/cm² of PTPAn loading, the Zn/PTPAn cell having $\text{Zn}(\text{OTf})_2\text{-TEP:PC}$ (1:2) electrolyte delivered maximum capacity of 85 mAh/g and average discharge voltage of ~ 1.5 V at 0.1 A/g. Further, at high PTPAn loading (8 mg/cm²) and high current density (1 A/g), the cell perfectly retained capacity, which lasted for 4,000 cycles.

Despite organic cathodes display outstanding rate performance and flexible operating temperature, their practical application is still hindered by their low electronic conductivity.^[87] Thus, large amount of conductive carbon should be added to the electrode to enhance their bulk electronic conductivity.

4.6. Graphite cathodes

The charge-storage mechanism of a graphite cathode in a dual-ion battery relies on the intercalation (charging)/deintercalation (discharging) of the anion i.e., PF_6^- , TFSI^- and OTF^- .^[16e,f,33a] Accordingly, the graphite cathode having anion intercalation exhibited very high voltage (> 2.0 V vs. Zn/Zn^{2+}); thus, high stability electrolytes such as organic electrolytes and RTIL electrolytes are required. Fan et al. (2019)^[16e] put forward a Zn/graphite cell having $\text{Zn}(\text{OTf})_2\text{-[EMIm]OTf}$ electrolyte. Via 0.2 M $\text{Zn}(\text{OTf})_2$ electrolyte, maximum capacity and discharge voltage was found to be 33.7 mAh/g and 2.0 V ($0.2 \text{ mA}/\text{cm}^2 \approx 154 \text{ mA}/\text{g}$), respectively. At 0.5 mA/cm² ($\sim 385 \text{ mA}/\text{g}$), capacity dropped to 22.4 mAh/g. The cell was seen to run for at least 100 cycles. However, a clear capacity drop was observed upon cycling at 0.2 mA/cm².

Zhang et al. (2019)^[16f] introduced the use of $\text{Zn}(\text{TFSI})_2\text{-AN}$ on a Zn/graphite cell (Figure 18a). After 10 cycles passed (50 mA/g), the capacity stabilized at 47.5 mAh/g, yielding the average discharge voltage of 2.2 V. The cell also exhibited excellent cyclability (82% capacity retention after 4,000 cycles at 1.0 A/g) and superior rate capability (Figure 18b and c); there was only a negligible capacity drop upon the current density range of 0.1 A/g to 1.5 A/g.

As proposed by Ji et al. (2020),^[33a] another Zn/graphite cell was carried out using $\text{Zn}(\text{TFSI})_2\text{-[C4mpyrr]TFSI}$ electrolyte. Thus, it was found that the reversible discharge capacity and the average discharge voltage was 57 mAh/g and 1.6 V (at 2 C ≈ 200 mA/g), respectively. The cell displayed 86% capacity retention after passing 500 cycles.

5. Perspective and Summary

This review highlights the application of nonaqueous electrolytes and NAQ-GPEs i.e., organic electrolytes, RTIL electrolytes and DES electrolytes in rechargeable ZIBs. The main reason for using nonaqueous electrolytes in improving ZIBs is due to their high electrochemical stability and gas production inhibition e.g., H_2 evolution and Zn self-corrosion, which allows the use of high voltage cathode (> 2 V vs. Zn/Zn^{2+} upon charging) such as spinel LiMn_2O_4 , polyanionic compound, cobalt oxide, Prussian blue and graphite, demonstrating little degradation upon cycling. In addition, it is noted that most nonaqueous electrolytes can significantly suppress dendrite formation on the Zn anode which is one of the most critical issues in ZIB development and can provide long-life Zn anode cycling. At this point, nonaqueous electrolytes appear to be an ideal choice for ZIB electrolytes. Nevertheless, there are several issues

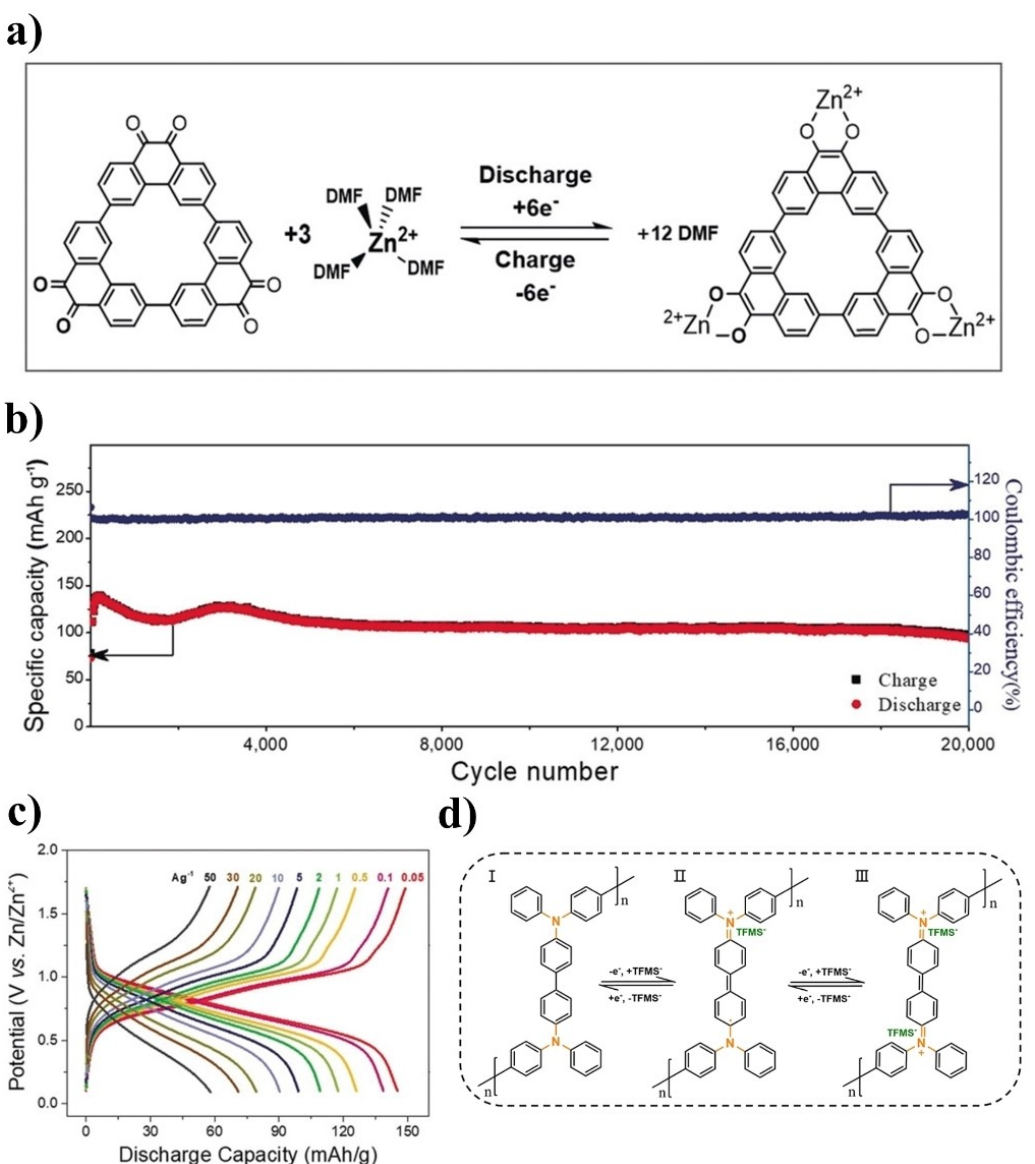


Figure 17. a–c) Zn/PQ-MCT battery ($Zn(OTf)_2$ -DMF): a) Schema of the charge-storage mechanisms of PQ-MCT cathode, b) cyclability results of Zn/PQ-MCT cell at 1 A/g, c) rate capability results of Zn/PQ-MCT cell.^[15a] Reproduced with permission from Ref. [15a]. Copyright (2020) Wiley-VCH. d) Schema of the charge-storage mechanisms of PTPAn cathode.^[23] Reproduced with permission from Ref. [23]. Copyright (2021) Wiley-VCH.

that need resolving for nonaqueous electrolytes to be applied on a practical scale.

In Figure 19, the plots of specific power versus specific energy of cathode materials conducted in nonaqueous media are illustrated. Herein, it is seen that published cathode-electrolyte systems cover a wide range of operations, and have a specific energy range (lower than 100 Wh/kg to higher than 300 Wh/kg). Of all cathode materials, $ZnNi_{1/2}Mn_{1/2}Co_4$ and the CoHcf demonstrate the highest energy density (> 300 Wh/kg). However, most of the systems provide the best performance (both in terms of power and energy) at around 1 C discharging rate, which indicates the moderate intercalation kinetics of NZIBs. Although high voltage cathodes are now available for ZIBs, they are quite slow in terms of rate capability compared to AZIBs. It is acknowledged that the ionic conductivity of

nonaqueous electrolytes such as organic electrolytes are in the range of 10^{-3} to 10^{-2} S/cm, which are not much different from aqueous electrolytes. The main issue that diminishes the kinetic of Zn^{2+} charge-storage reaction is the high desolvation penalty that occurred due to the strong interaction between the Zn^{2+} and other electrolyte components (i.e., anion and solvent molecule). Therefore, to enhance the performance of NZIB, it does not only require electrolyte development but also requires host material development.

For this purpose, the rational design of the electrolyte or fine-tuning via cosolvents can minimize the effect of anion-cation pairing. Another viable approach is to tune the surface chemistry of the host material to support the solvation of guest ions. To date, the most straightforward approach to improve NZIB performance is the addition of water; the addition of

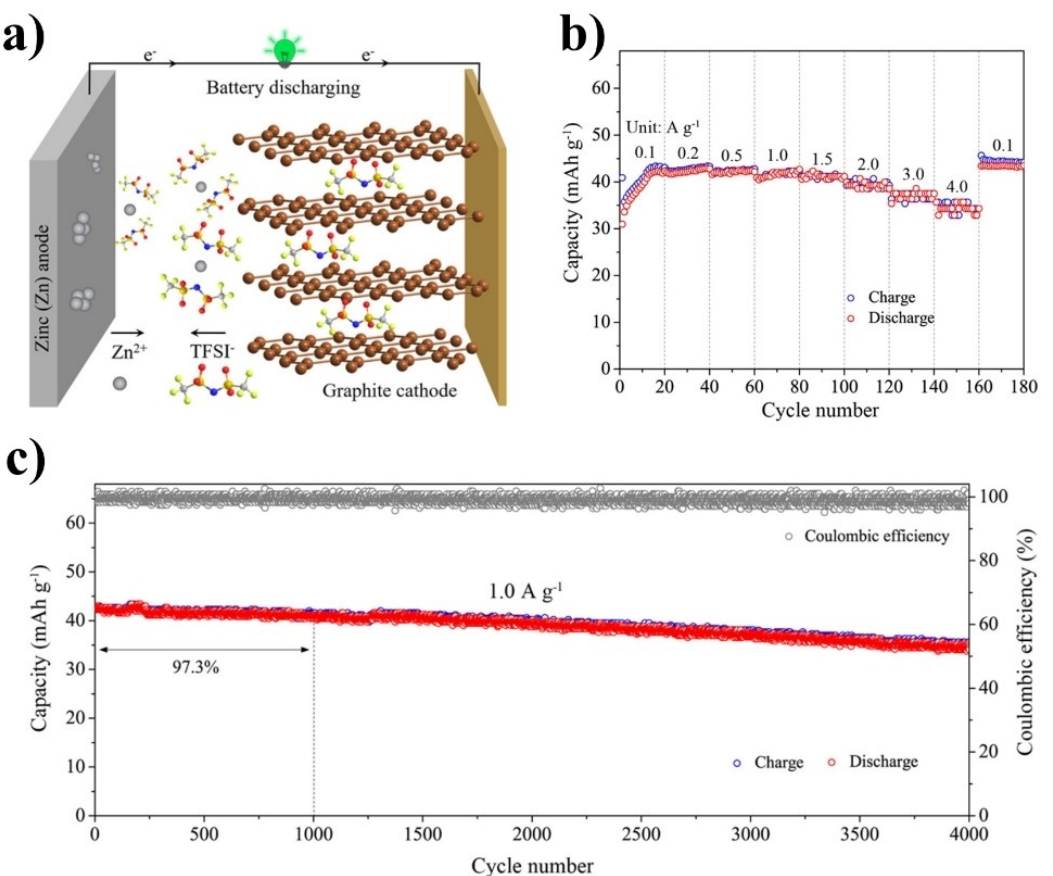


Figure 18. Electrochemical performance of Zn/graphite cell having $Zn(TFSI)_2$ -AN electrolyte: a) Schema of the charge-storage reaction of Zn/graphite cell. b) Rate capability results of Zn/graphite cell. c) Cyclability results of Zn/graphite cell at 1 A/g.^[16f] Reproduced with permission from Ref. [16f]. Copyright (2019) American Chemical Society.

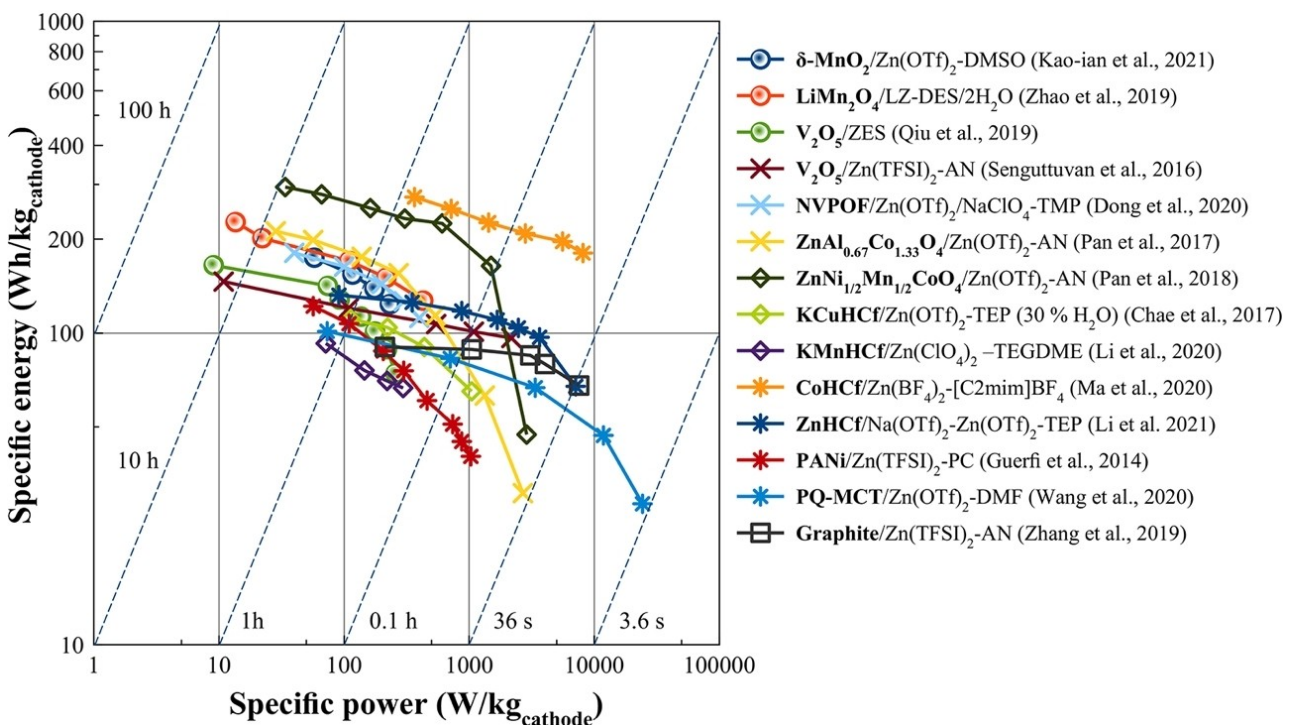


Figure 19. Ragone plots of NZIBs (normalized by weight of cathode material).^[9,13,15,16b-d,f,18e,f,19,20,31b,37]

water not only enhances the ionic conductivity, but also increases the rate performance of the battery. Water added to the electrolyte acts like a "lubricant" to drive the insertion reaction. However, complete understanding regarding the intrinsic role of water has yet to be elucidated. Furthermore, some works indicate that the hybrid (dual-ion) system, which utilizes the advance of the monovalent ion (i.e., K^+ , Li^+ and Na^+), is one of the possible approaches to enhance the cell voltage and rate capability of the battery. Those monovalent cations face fewer problems regarding poor diffusion and electrostatic interaction than Zn^{2+} cation.

Several research groups have demonstrated satisfactory results when Zn anodes have been applied using nonaqueous electrolytes. However, more substantiation is required to ensure their practical application. Ma et al. (2020)^[88] stated that an ideal target for Zn anode towards commercialization is 5 mAh/cm² areal capacity having 100% CE, which can last for 2,000 cycles; the Zn anode should be capable enough to hold against the high charging rate (2 C, 10 mA/cm²). To achieve such a goal, it is important to recognize the current status of the Zn anode within nonaqueous ZIB research. In Table 5, the data regarding Zn anode rechargeability in nonaqueous media gathered from this review is shown. It is seen that there are only two systems viz. $Zn(OTf)_2$ -TEP and $Zn(OTf)_2$ -TMP that can meet the target of 5 mAh/cm² areal capacity. Yet neither of these can operate at high current of 10 mA/cm². In Section 3 of

this review, the $Zn(OTf)_2/Zn(TFSI)_2$ -AN and $Zn(BF_4)_2/[C2mim]BF_4$ can hit 10 mA/cm² current density, but only 0.4 and 0.5 mAh testing capacity was used, respectively. Overall, it is evident that there are limits in terms of the plating/stripping kinetics of Zn in nonaqueous media, and as such require further improvement. Possible strategies that can be undertaken to surpass this goal include 1) the development of the solid electrolyte interface (SEI) that can reduce energy loss due to the desolvation penalty and 2) the electrolyte design to reduce the effect of anion-cation pairing.

In terms of CE, most Zn-nonaqueous systems provide positively good results (> 99%). Such results are due to the stability of nonaqueous electrolytes. However, it is found that none of the works presented herein can perform higher than 10% depth of discharge (DOD). This means that more than 90% of unused Zn still existed in the cell. This excessive amount of Zn may well lead to the low energy density of the full cell. Thus, the effects of DOD should be further investigated.

In addition, some groups have chosen CV test to evaluate the reversibility of the anode. However, CV results possess a limitation regarding controlling the charge-transfer amount. In addition, the potential window used in the CV test is not fit an actual operation of the anode in a real battery. Therefore, it is suggested that the use of GCD on the anode test is more suitable for this purpose.

Table 5. Zn anode performance evaluated using GCD tests

Electrolytes	CE [CC/Zn cell]	Maximum cycling time [Zn/Zn cell]	Testing capacity	Anode type	DOD (each cycle)	Ref.
0.5 M $Zn(TFSI)_2$ -AN	99.80%	~300 h (1.25 mA/cm ²)	0.408 mAh/cm ²	Zn foil (thickness: 0.25 mm, ~146.2 mAh/cm ²)	0.28%	[18a]
0.5 M $Zn(OTf)_2$ -AN	99.90%	~400 h (1.25 mA/cm ²)	0.408 mAh/cm ²	Zn foil (thickness: 0.25 mm, ~146.2 mAh/cm ²)	0.28%	[18a]
1 M $Zn(TFSI)_2$ -AN	99.50%	1000 h (0.5 mA/cm ²)	0.25 mAh/cm ²	Zn foil	N/A	[16f]
0.5 M $Zn(TFSI)_2$ -PC**	99.1% **	9 cycles (0.5 mA/cm ²)**	1 mAh/cm ² **	Zn on Cu: 5 mAh/cm ² **	N/A	[65]
0.5 M $Zn(OTf)_2$ -DMF	99.8%	2800 h (1.0 mA/cm ²)	1 mAh/cm ²	Zn foil (t: 0.03 mm, ~17.5 mAh/cm ²)	5.71%	[15a]
0.5 $Zn(OTf)_2$ -TEP	99.86%	3000 h (0.1–0.5 mA/cm ²)	0.1–0.5 mAh/cm ²	Zn foil (t: 0.25 mm, ~146.2 mAh/cm ²)	0.07–0.34 %	[16a]
		2000 h (0.5 mA/cm ²)	5 mAh/cm ²	Zn foil (t: 0.25 mm, ~146.2 mAh/cm ²)	3.42%	
0.5 M $Zn(OTf)_2$ -TMP	99.57%	>2300 h (0.1–1.0 mA/cm ²)	0.1–0.5 mAh/cm ²	Zn foil	N/A	[21]
		1000 h (0.5–1 mA/cm ²)	5–10 mAh/cm ²	Zn foil (t: 0.25 mm, ~146.2 mAh/cm ²)	3.42–6.84 %	
0.5 M/1.0 M of $Zn(OTf)_2$ /NaClO ₄ -TMP	99.80%	5000 h (0.5 mA/cm ²)	0.25 mAh/cm ²	Zn foil	N/A	[16d]
0.25 M $Zn(OTf)_2$ -DMSO	99.60%	>100 h (0.1–1.0 mA/cm ²)	0.025–0.25 mAh/cm ²	Zn foil (t: 0.10 mm, 58.5 mAh/cm ²)	0.04–0.43 %	[9]
0.5 $Zn(OTf)_2$ -TEP:PC	99.70%	2600 h (0.5 mA/cm ²)	0.5 mAh/cm ²	Zn foil (t: 0.03 mm, ~17.5 mAh/cm ²)	2.86 %	[23]
0.5 M $Zn(OTf)_2$ -TMP:DMC	99.15 %	>5000 h (1.0 mA/cm ²)	1 mAh/cm ²	Zn foil	N/A	[21]
9 mol% $Zn(dca)_2$ -[C2mim] dca (3 wt.% water)	85 %	375 h (0.1 mA/cm ²)	0.2 mAh/cm ²	Zn foil	N/A	[27]
2 M $Zn(BF_4)_2$ -[C2mim]BF ₄	99.36 %	1500 h (2 mA/cm ²)	0.5 mAh/cm ²	Zn foil	N/A	[13]
9 mol% $Zn(dca)_2$ -[C4mpyrr] dca (3 wt.% water)	37 %	60 h (0.05 mA/cm ²)	0.05 mAh/cm ²	Zn foil	N/A	[27]
ZES	99.70%	2000 h (0.1 mA/cm ²)	0.05 mAh/cm ²	Zn foil (11.7 mAh/cm ²)	0.43 %	[31b]
		100 h (0.1 mA/cm ²)	0.5 mAh/cm ²	Zn foil (11.7 mAh/cm ²)	4.27 %	
LZ-DES/2H ₂ O	96.20%	2400 h (0.1 mA/cm ²)	0.074 mA/cm ²	Zn foil (11.2 mAh/cm ²)	0.66 %	[37]

Regarding safety, the use of organic electrolytes tends to have a higher risk of flammability than that of aqueous electrolytes. Nevertheless, strategies have been developed in LIB research that is open for the implementation of the ZIB, such as the addition of fire retardant and the addition of overcharge additives.^[53] In addition, the use of ionic liquid and the ionic liquid-based GPE, which is fundamentally safe to the flame, is also one of the possible ways to enhance safety.

In conclusion, nonaqueous electrolytes are a promising alternative system that can enhance the stability of the ZIBs. Although NZIBs cannot provide comparable power density as AZIBs, such drawbacks can be compensated with the higher stability of the Zn anode and the H₂-free property. However, to meet the practical need, further research to improve the performance, cyclability and safety for the NZIBs are required. In addition, standard or proper testing protocols should be established.

Acknowledgements

National Science and Technology Development Agency through the Southeast Asia-Europe Joint Funding Scheme for Research and Innovation (FDA-CO-2563-11897-TH), The Program Unit for Human Resources & Institutional Development, Research and Innovation (B16F640166), and the Energy Storage Cluster, Chulalongkorn University are acknowledged. W.K. and S.K. thank the support from the Royal Golden Jubilee Ph.D. Program, Thailand. A.A.M thanks the finance support from NIPPON SHEET GLASS 2021 (304.PBAHAN.6050464.N120). W.L. gratefully acknowledged to Ministry of Science and Technology, Taiwan, project grant Nos. MOST 109-2923-E-006-006, 110-2622-M-033-001, 109-2622-E-033-010, 110-2923-E-006-011, 110-3116-F-011-002 and 108-E-033-MY3.

Conflict of Interest

The authors declare no conflict of interest.

Keywords: costs • deep eutectic solvent • ionic liquid • non-proton donor electrolyte • organic

- [1] Y. Zhang, Z. Chen, H. Qiu, W. Yang, Z. Zhao, J. Zhao, G. Cui, *NPG Asia Mater.* **2020**, *12*, 4.
- [2] L. E. Blanc, D. Kundu, L. F. Nazar, *Joule* **2020**, *4*, 771.
- [3] J. Ming, J. Guo, C. Xia, W. Wang, H. N. Alshareef, *Mater. Sci. Eng. R* **2019**, *135*, 58–84.
- [4] C. Xu, B. Li, H. Du, F. Kang, *Angew. Chem. Int. Ed.* **2012**, *51*, 933.
- [5] T. Zhang, Y. Tang, S. Guo, X. Cao, A. Pan, G. Fang, J. Zhou, S. Liang, *Energy Environ. Sci.* **2020**, *13*, 4625.
- [6] W. Zhang, S. Liang, G. Fang, Y. Yang, J. Zhou, *Nano-Micro Lett.* **2019**, *11*, 69.
- [7] N. Wang, H. Wan, J. Duan, X. Wang, L. Tao, J. Zhang, H. Wang, *Mater. Today* **2021**, *11*, 100149.
- [8] a) X. Zhu, Z. Cao, W. Wang, H. Li, J. Dong, S. Gao, D. Xu, L. Li, J. Shen, M. Ye, *ACS Nano* **2021**, *15*, 2971; b) T. Xue, H. J. Fan, *J. Energy Chem.* **2021**, *54*, 194; c) X. Jia, C. Liu, Z. G. Neale, J. Yang, G. Cao, *Chem. Rev.* **2020**, *120*, 7795–7866.
- [9] W. Kao-ian, M. T. Nguyen, T. Yonezawa, R. Pornprasertsuk, J. Qin, S. Siwamogsatham, S. Kheawhom, *Mater. Today* **2021**, *100738*.
- [10] C. Xie, Y. Li, Q. Wang, D. Sun, Y. Tang, H. Wang, *Carbon Energy* **2020**, *2*, 540.
- [11] a) H. Liu, Y. Zhang, C. Wang, J. N. Glazer, Z. Shan, N. Liu, *ACS Appl. Mater. Interfaces* **2021**, *13*, 32930; b) X. Guo, Z. Zhang, J. Li, N. Luo, G.-L. Chai, T. S. Miller, F. Lai, P. Shearing, D. J. L. Brett, D. Han, Z. Weng, G. He, I. P. Parkin, *ACS Energy Lett.* **2021**, *6*, 395.
- [12] a) J. Hao, X. Li, S. Zhang, F. Yang, X. Zeng, S. Zhang, G. Bo, C. Wang, Z. Guo, *Adv. Funct. Mater.* **2020**, *30*, 2001263; b) L. Lei, Y. Sun, X. Wang, Y. Jiang, J. Li, *Front. Mater.* **2020**, *7*.
- [13] L. Ma, S. Chen, N. Li, Z. Liu, Z. Tang, J. A. Zapien, S. Chen, J. Fan, C. Zhi, *Adv. Mater.* **2020**, *32*, 1908121.
- [14] a) Q. Li, J. Chen, L. Fan, X. Kong, Y. Lu, *Green Energy & Environ.* **2016**, *1*, 18; b) N. Nitta, F. Wu, J. T. Lee, G. Yushin, *Mater. Today* **2015**, *18*, 252.
- [15] a) N. Wang, X. Dong, B. Wang, Z. Guo, Z. Wang, R. Wang, X. Qiu, Y. Wang, *Angew. Chem. Int. Ed.* **2020**, *59*, 14577; b) Q. Li, K. Ma, G. Yang, C. Wang, *Energy Storage Mater.* **2020**, *29*, 246.
- [16] a) A. Naveed, H. Yang, J. Yang, Y. Nuli, J. Wang, *Angew. Chem. Int. Ed.* **2019**, *58*, 2760; b) C. Pan, R. G. Nuzzo, A. A. Gewirth, *Chem. Mater.* **2017**, *29*, 9351; c) C. Pan, R. Zhang, R. G. Nuzzo, A. A. Gewirth, *Adv. Energy Mater.* **2018**, *8*, 1800589; d) Y. Dong, S. Di, F. Zhang, X. Bian, Y. Wang, J. Xu, L. Wang, F. Cheng, N. Zhang, *J. Mater. Chem. A* **2020**, *8*, 3252; e) J. Fan, Q. Xiao, Y. Fang, L. Li, W. Yuan, *Ionics* **2019**, *25*, 1303–1313; f) N. Zhang, Y. Dong, Y. Wang, Y. Wang, J. Li, J. Xu, Y. Liu, L. Jiao, F. Cheng, *ACS Appl. Mater. Interfaces* **2019**, *11*, 32978.
- [17] S.-D. Han, N. N. Rajput, X. Qu, B. Pan, M. He, M. S. Ferrandon, C. Liao, K. A. Persson, A. K. Burrell, *ACS Appl. Mater. Interfaces* **2016**, *8*, 3021.
- [18] a) A. S. Etman, M. Carboni, J. Sun, R. Younesi, *Energy Technol.* **2020**, *8*, 2000358; b) D. Kundu, S. Hosseini Vajargah, L. Wan, B. Adams, D. Prendergast, L. F. Nazar, *Energy Environ. Sci.* **2018**, *11*, 881; c) V. Verma, S. Kumar, W. Manalastas, J. Zhao, R. Chua, S. Meng, P. Kidkhunthod, M. Srinivasan, *ACS Appl. Mater. Interfaces* **2019**, *2*, 8667; d) S.-D. Han, S. Kim, D. Li, V. Petkov, H. D. Yoo, P. J. Phillips, H. Wang, J. J. Kim, K. L. More, B. Key, R. F. Klie, J. Cabana, V. R. Stamenkovic, T. T. Fister, N. M. Markovic, A. K. Burrell, S. Tepeavcevic, J. T. Vaughey, *Chem. Mater.* **2017**, *29*, 4874; e) M. S. Chae, J. W. Heo, H. H. Kwak, H. Lee, S.-T. Hong, *J. Power Sources* **2017**, *337*, 204; f) P. Senguttuvan, S.-D. Han, S. Kim, A. L. Lipson, S. Tepeavcevic, T. T. Fister, I. D. Bloom, A. K. Burrell, C. S. Johnson, *Adv. Energy Mater.* **2016**, *6*, 1600826.
- [19] A. Guerfi, J. Trottier, I. Boyano, I. De Meazza, J. A. Blazquez, S. Brewer, K. S. Ryder, A. Vijh, K. Zaghib, *J. Power Sources* **2014**, *248*, 1099.
- [20] Q. Li, K. Ma, C. Hong, Z. Yang, C. Qi, G. Yang, C. Wang, *Energy Storage Mater.* **2021**, *42*, 715.
- [21] A. Naveed, H. Yang, Y. Shao, J. Yang, N. Yanna, J. Liu, S. Shi, L. Zhang, A. Ye, B. He, J. Wang, *Adv. Mater.* **2019**, *31*, 1900668.
- [22] R. D. Corpuz, L. M. De Juan-Corpuz, M. T. Nguyen, T. Yonezawa, H.-L. Wu, A. Somwangthanaroj, S. Kheawhom, *Int. J. Mol. Sci.* **2020**, *21*, 3113.
- [23] X. Qiu, N. Wang, X. Dong, J. Xu, K. Zhou, W. Li, Y. Wang, *Angew. Chem. Int. Ed.* **2021**, *60*, 21025.
- [24] G. M. Asselin, O. Paden, W. Qiu, Z. Yang, N. Sa, *J. Electrochem. Soc.* **2021**, *168*, 030516.
- [25] A. M. O'Mahony, D. S. Silvester, L. Aldous, C. Hardacre, R. G. Compton, *J. Chem. Eng. Data* **2008**, *53*, 2884.
- [26] G. Damilano, D. Kalebić, K. Binnemans, W. Dehaen, *RSC Adv.* **2020**, *10*, 21071–21081.
- [27] T. J. Simons, D. R. MacFarlane, M. Forsyth, P. C. Howlett, *ChemElectroChem* **2014**, *1*, 1688.
- [28] a) L. Zhang, G. Wang, J. Feng, Q. Ma, Z. Liu, X. Yan, *ChemElectroChem* **2021**, *8*, 1289; b) M. S. Ghazvini, G. Pulletkurthi, A. Lahiri, F. Endres, *ChemElectroChem* **2016**, *3*, 598–604.
- [29] a) M. Kar, C. Pozo-Gonzalo, *Curr. Opin. Green Sustain. Chem.* **2021**, *28*, 100426; b) G. García, S. Aparicio, R. Ullah, M. Atilhan, *Energy Fuels* **2015**, *29*, 2616.
- [30] A. P. Abbott, G. Capper, D. L. Davies, R. K. Rasheed, V. Tambyrajah, *Chem. Commun.* **2003**, *70*.
- [31] a) E. L. Smith, A. P. Abbott, K. S. Ryder, *Chem. Rev.* **2014**, *114*, 11060–11082; b) H. Qiu, X. Du, J. Zhao, Y. Wang, J. Ju, Z. Chen, Z. Hu, D. Yan, X. Zhou, G. Cui, *Nat. Commun.* **2019**, *10*, 5374.
- [32] a) T. J. Simons, P. C. Howlett, A. A. J. Torriero, D. R. MacFarlane, M. Forsyth, *J. Phys. Chem. C* **2013**, *117*, 2662; b) T. J. Simons, A. A. J. Torriero, P. C. Howlett, D. R. MacFarlane, M. Forsyth, *Electrochim. Commun.* **2012**, *18*, 119.
- [33] a) B. Ji, W. Yao, Y. Tang, *Sustain. Energy Fuels* **2020**, *4*, 101; b) B. Dilasari, Y. Jung, K. Kwon, *J. Ind. Eng. Chem.* **2017**, *45*, 375; c) M. Xu, D. G. Ivey, Z.

- Xie, W. Qu, E. Dy, *Electrochim. Acta* **2013**, *97*, 289; d) K. R. Harris, L. A. Woolf, M. Kanakubo, T. Rüther, *J. Chem. Eng. Data* **2011**, *56*, 4672.
- [34] T. J. Simons, P. M. Bayley, Z. Zhang, P. C. Howlett, D. R. MacFarlane, L. A. Madson, M. Forsyth, *J. Phys. Chem. B* **2014**, *118*, 4895.
- [35] a) W. Kao-ian, R. Pornprasertsuk, P. Thamyongkit, T. Maiyalagan, S. Kheawhom, *J. Electrochem. Soc.* **2019**, *166*, A1063; b) C. Du, B. Zhao, X.-B. Chen, N. Birbilis, H. Yang, *Sci. Rep.* **2016**, *6*, 29225.
- [36] N. S. Venkata Narayanan, B. V. Ashokraj, S. Sampath, *J. Colloid Interface Sci.* **2010**, *342*, 505.
- [37] J. Zhao, J. Zhang, W. Yang, B. Chen, Z. Zhao, H. Qiu, S. Dong, X. Zhou, G. Cui, L. Chen, *Nano Energy* **2019**, *57*, 625.
- [38] a) S. Lorca, F. Santos, A. J. Fernández Romero, *Polymer* **2020**, *12*, 2812; b) F. Ilyas, M. Ishaq, M. Jabeen, M. Saeed, A. Ihsan, M. Ahmed, *J. Mol. Liq.* **2021**, *343*, 117606.
- [39] E. J. Hansen, J. Liu, *Front. Energy Res.* **2021**, *8*, 616665.
- [40] J. P. Tafur, J. Abad, E. Román, A. J. Fernández Romero, *Electrochem. Commun.* **2015**, *60*, 190.
- [41] K. Ylli, D. Hoffmann, A. Willmann, Y. Manoli, *J. Phys. Conf. Ser.* **2018**, *1052*, 012085.
- [42] C. M. S. Prasanna, S. A. Suthanthiraraj, *J. Polym. Res.* **2016**, *23*, 1.
- [43] R. Rathika, S. A. Suthanthiraraj, *J. Mater. Sci. Mater. Electron.* **2018**, *29*, 19632.
- [44] J. P. Tafur, F. Santos, A. J. F. Romero, *Membranes* **2015**, *5*, 752–771.
- [45] J. P. T. Guisao, A. J. F. Romero, *Electrochim. Acta* **2015**, *176*, 1447.
- [46] J. J. Xu, H. Ye, J. Huang, *Electrochem. Commun.* **2005**, *7*, 1309.
- [47] K. Sowthari, S. Austin Suthanthiraraj, *J. Phys. Chem. Solids* **2014**, *75*, 746.
- [48] S. P. Candhadai Murali, A. S. Samuel, *J. Appl. Polym. Sci.* **2019**, *136*, 47654.
- [49] H. Ye, J. J. Xu, *J. Power Sources* **2007**, *165*, 500.
- [50] G. G. Kumar, S. Sampath, *J. Electrochem. Soc.* **2003**, *150*, A608.
- [51] Sellam, S. A. Hashmi, *J. Solid State Electrochem.* **2012**, *16*, 3105.
- [52] E. P. Roth, C. J. Orendorff, *Electrochem. Soc. Interface* **2012**, *21*, 45.
- [53] Q. Wang, L. Jiang, Y. Yu, J. Sun, *Nano Energy* **2019**, *55*, 93.
- [54] J. Shi, K. Xia, L. Liu, C. Liu, Q. Zhang, L. Li, X. Zhou, J. Liang, Z. Tao, *Electrochim. Acta* **2020**, *358*, 136937.
- [55] National Center for Biotechnology Information advances science and health, "Acetonitrile", can be found under <https://pubchem.ncbi.nlm.nih.gov/compound/Acetonitrile>, 2022.
- [56] National Center for Biotechnology Information advances science and health, "Diglyme", can be found under <https://pubchem.ncbi.nlm.nih.gov/compound/Diglyme>, 2022.
- [57] National Center for Biotechnology Information advances science and health, "Propylene carbonate", can be found under <https://pubchem.ncbi.nlm.nih.gov/compound/Propylene-carbonate>, 2022.
- [58] National Center for Biotechnology Information advances science and health, "N,N-dimethylformamide", can be found under <https://pubchem.ncbi.nlm.nih.gov/compound/N,N-dimethylformamide>, 2022.
- [59] National Center for Biotechnology Information advances science and health, "Triethyl phosphate", can be found under <https://pubchem.ncbi.nlm.nih.gov/compound/Triethyl-phosphate>, 2022.
- [60] National Center for Biotechnology Information advances science and health, "Trimethyl phosphate", can be found under <https://pubchem.ncbi.nlm.nih.gov/compound/Trimethyl-phosphate>, 2022.
- [61] Merck, "Tetraethylene glycol dimethyl ether", can be found under <https://www.merckmillipore.com/TH/en/product/Tetraethylene-glycol-dimethyl-ether>, MDA_CHEM-820959, 2022.
- [62] National Center for Biotechnology Information advances science and health, "Dimethyl sulfoxide", can be found under <https://pubchem.ncbi.nlm.nih.gov/compound/Dimethyl-sulfoxide>, 2022.
- [63] National Center for Biotechnology Information advances science and health, "Tetrahydrofuran", can be found under <https://pubchem.ncbi.nlm.nih.gov/compound/Tetrahydrofuran>, 2022.
- [64] J. Xie, Y.-C. Lu, *Nat. Commun.* **2020**, *11*, 2499.
- [65] L. Ma, M. A. Schroeder, T. P. Pollard, O. Borodin, M. S. Ding, R. Sun, L. Cao, J. Ho, D. R. Baker, C. Wang, K. Xu, *Energy Environ. Mater.* **2020**, *3*, 516.
- [66] D. Chen, X. Rui, Q. Zhang, H. Geng, L. Gan, W. Zhang, C. Li, S. Huang, Y. Yu, *Nano Energy* **2019**, *60*, 171.
- [67] S. Asha, K. P. Vijayalakshmi, B. K. George, *Int. J. Quantum Chem.* **2019**, *119*, e26014.
- [68] M.-J. Deng, P.-C. Lin, J.-K. Chang, J.-M. Chen, K.-T. Lu, *Electrochim. Acta* **2011**, *56*, 6071.
- [69] a) A. P. Abbott, J. C. Barron, G. Frisch, S. Gurman, K. S. Ryder, A. Fernando Silva, *Phys. Chem. Chem. Phys.* **2011**, *13*, 10224; b) R. Bernasconi, G. Panzeri, G. Firtin, B. Kahyaoglu, L. Nobili, L. Magagnin, *J. Phys. Chem. B* **2020**, *124*, 10739; c) L. Vieira, R. Schennach, B. Gollas, *Electrochim. Acta* **2016**, *197*, 344.
- [70] N. M. Pereira, C. M. Pereira, J. P. Araújo, A. Fernando Silva, *J. Electroanal. Chem.* **2017**, *801*, 545.
- [71] M. Metzger, J. Sicklinger, D. Haering, C. Kavaklı, C. Stinner, C. Marino, H. A. Gasteiger, *J. Electrochem. Soc.* **2015**, *162*, A1227.
- [72] H. Yang, R. G. Reddy, *Electrochim. Acta* **2014**, *147*, 513.
- [73] X. Guo, S. Yang, D. Wang, A. Chen, Y. Wang, P. Li, G. Liang, C. Zhi, *Curr. Opin. Electrochem.* **2021**, *30*, 100769.
- [74] R. D. Corpuz, L. M. Z. De Juan, S. Praserthdam, R. Pornprasertsuk, T. Yonezawa, M. T. Nguyen, S. Kheawhom, *Sci. Rep.* **2019**, *9*, 15107.
- [75] a) J. Shin, J. K. Seo, R. Yaylian, A. Huang, Y. S. Meng, *Int. Mater. Rev.* **2020**, *65*, 356; b) S. Khamnsanga, R. Pornprasertsuk, T. Yonezawa, A. A. Mohamad, S. Kheawhom, *Sci. Rep.* **2019**, *9*, 8441; c) S. Khamnsanga, M. T. Nguyen, T. Yonezawa, P. Thamyongkit, R. Pornprasertsuk, P. Pattananuwat, A. Tuantranont, S. Siwamogsatham, S. Kheawhom, *Int. J. Mol. Sci.* **2020**, *21*, 4689.
- [76] D. A. Kitchev, H. Peng, Y. Liu, J. Sun, J. P. Perdew, G. Ceder, *Phys. Rev. B* **2016**, *93*, 045132.
- [77] Y. Xie, Y. Jin, L. Xiang, *Crystals* **2017**, *7*, 221.
- [78] N. Nakayama, T. Nozawa, Y. Iriyama, T. Abe, Z. Ogumi, K. Kikuchi, *J. Power Sources* **2007**, *174*, 695.
- [79] T. Zhang, D. Li, Z. Tao, J. Chen, *Prog. Nat. Sci.* **2013**, *23*, 256.
- [80] L. M. De Juan-Corpuz, R. D. Corpuz, A. Somwangthanaroj, M. T. Nguyen, T. Yonezawa, J. Ma, S. Kheawhom, *Energies* **2020**, *13*, 31.
- [81] a) N. Zhang, Y. Dong, M. Jia, X. Bian, Y. Wang, M. Qiu, J. Xu, Y. Liu, L. Jiao, F. Cheng, *ACS Energy Lett.* **2018**, *3*, 1366; b) J. Zhou, L. Shan, Z. Wu, X. Guo, G. Fang, S. Liang, *Chem. Commun.* **2018**, *54*, 4457.
- [82] P. He, M. Yan, G. Zhang, R. Sun, L. Chen, Q. An, L. Mai, *Adv. Energy Mater.* **2017**, *7*, 1601920.
- [83] G. Li, Z. Yang, Y. Jiang, C. Jin, W. Huang, X. Ding, Y. Huang, *Nano Energy* **2016**, *25*, 211–217.
- [84] J.-Z. Guo, P.-F. Wang, X.-L. Wu, X.-H. Zhang, Q. Yan, H. Chen, J.-P. Zhang, Y.-G. Guo, *Adv. Mater.* **2017**, *29*, 1701968.
- [85] Y. Lyu, X. Wu, K. Wang, Z. Feng, T. Cheng, Y. Liu, M. Wang, R. Chen, L. Xu, J. Zhou, Y. Lu, B. Guo, *Adv. Energy Mater.* **2021**, *11*, 2000982.
- [86] F. Cheng, W. Tang, C. Li, J. Chen, H. Liu, P. Shen, S. Dou, *Chem. Eur. J.* **2006**, *12*, 3082.
- [87] a) S. Xu, M. Sun, Q. Wang, C. Wang, *J. Semiconductors* **2020**, *41*, 091704; b) Q. Wang, X. Xu, G. Yang, Y. Liu, X. Yao, *Chem. Commun.* **2020**, *56*, 11859.
- [88] L. Ma, M. A. Schroeder, O. Borodin, T. P. Pollard, M. S. Ding, C. Wang, K. Xu, *Nat. Energy* **2020**, *5*, 743.

Manuscript received: November 23, 2021

Revised manuscript received: January 22, 2022

Accepted manuscript online: January 29, 2022

Version of record online: February 18, 2022